DOI: 10.1002/anie.200701111

Liquid Crystals

Transmission and Amplification of Information and Properties in Nanostructured Liquid Crystals**

John W. Goodby, Isabel M. Saez, Stephen J. Cowling, Verena Görtz, Michael Draper, Alan W. Hall, Susan Sia, Guirac Cosquer, Seung-Eun Lee, and E. Peter Raynes*

Keywords:
chirality · glycolipids · liquid crystals · self-assembly · supramolecular chemistry

In memory of Pierre-Gilles de Gennes

In recent years the design of chemical structures of liquid-crystalline materials has developed rapidly, and in many cases changed radically. Since Reinitzer's days, liquid crystals have either been classed as rodlike or disclike, with combinations of the two leading to phasmidic liquid crystals. The discovery that materials with bent molecular structures exhibited whole new families of mesophases inspired investigations into the liquid-crystal properties of materials with widely varying molecular topologies—from pyramids to crosses to dendritic molecules. As a result of conformational change, supermolecular materials can have deformable molecular structures, which can stabilize mesophase formation, and some materials that are non-mesogenic, on complexation form supramolecular liquid crystals. The formation of mesophases by individual molecular systems is a process of self-organization, whereas the mesophases of supramolecular systems are formed by self-assembly and self-organization. Herein we show 1) deformable molecular shapes and topologies of supermolecular and self-assembled supramolecular systems; 2) surface recognition processes of superstructures; and 3) that the transmission of those structures and their amplification can lead to unusual mesomorphic behavior where conventional continuum theory is not suitable for their description.

From the Contents

1. Introduction

The functional materials of living systems are based on supermolecular and supramolecular self-organizing and self-assembling systems of discrete structure and topology. The term supermolecular describes a giant molecule made up of covalently bound smaller identifiable components, and supramolecular means an identifiable system made up of multiple components that are not covalently bound together. For example, proteins, although peptide polymers, have defined and reproducible primary compositions of amino acids, specified α-helical and β-pleated secondary constructions, and gross topological tertiary structures. Moreover, highly specific functionality, and thereby the ability to perform selective chemical processing, is in-built into such molecular machines. Concomitantly, the study of materials that self-assemble into supramolecular structures with desirable functionality and physical properties at nano- and mesoscopic length scales is currently an exciting area of intense research, and provides a "bottom-up" approach to the design and synthesis of functional materials.

Liquid crystals, on the other hand, have become the quintessential self-organizing molecular materials of the modern era. They are often thought of as advanced technological materials which are found in high content, low power, flat-panel displays—known to the whole world as LCDs (liquid-crystal displays). However, even for those who are relatively familiar with the subject, it is not often appreciated that the term "liquid crystal" represents a collection of separate, identifiable, states of matter—"the fourth state of matter", which, like other states of matter, pervades all classes of low-molar-mass and polymeric materials, and touches upon a vast number of different, and at the same time, multidisciplinary topics of research, and a plethora of practical applications, from displays and electrooptic switches, to sensors, high-performance polymers, detergents, and drug-delivery vectors (Figure 1).[1]

In the early design of materials to exhibit thermotropic liquid-crystal phases, the shapes of the molecules were characterized as either rigid rods or discs (and spheres in terms of plastic crystals). Also for the most part, the study of small-molecular systems dominated the field. The accepted theory to depict and explain the physical properties of these liquid-crystalline systems then was, and to this date, still is that of the continuum theory. The continuum theory describes the

[*] Prof. J. W. Goodby, Dr. I. M. Saez, Dr. S. J. Cowling, Dr. V. Görtz, M. Draper, Dr. A. W. Hall, Dr. S. Sia
University of York
Department of Chemistry
York, YO10 5DD (UK)
Fax: (+44) 1904-432-516
E-mail: jwg500@york.ac.uk
Dr. G. Cosquer
Department of Chemistry, University of Hull
Cottingham Road, Hull, HU6 7RX (UK)
Dr. S.-E. Lee
R&D Technical Centre
Merck Advanced Technologies Ltd (South Korea)
Prof. E. P. Raynes
Department of Engineering, University of Oxford
Parks Road, Oxford, OX1 3PJ (UK)

[**] This article is based on a Plenary Lecture given by J. W. Goodby at the 21st International Liquid Crystal Conference, Keystone, Colorado, USA.

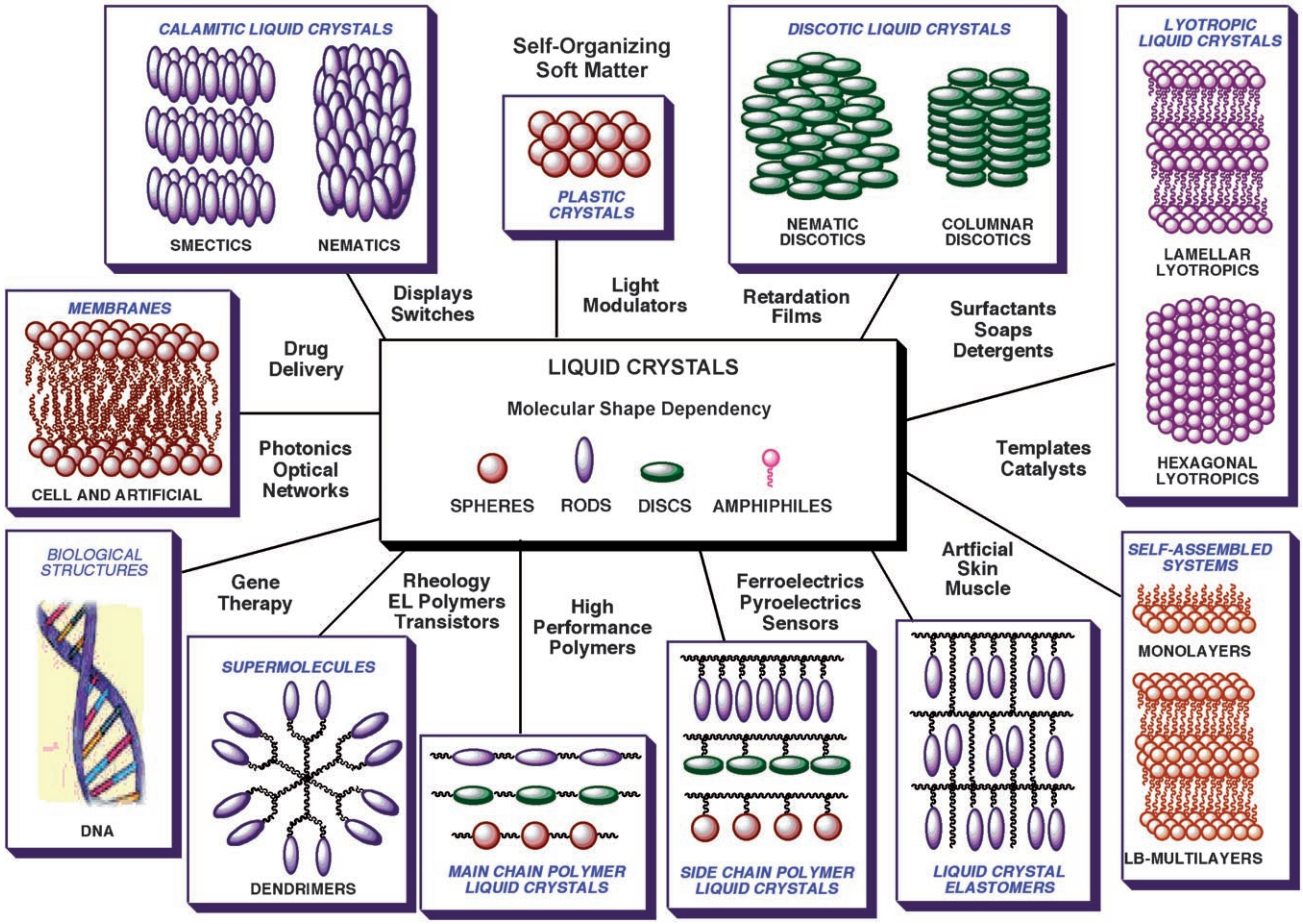

Figure 1. Classes of liquid crystals defined by molecular shape, the structures of their condensed phases, and their applications.

liquid-crystalline state as an anisotropic elastic fluid possessing its own symmetry, viscosity, and elasticity parameters.[2] Thus, the nematic phase, which is the least ordered and most fluid, in other words, the most liquid-like of the mesophases, is portrayed by the theory as being a homogeneous state of matter. The outstanding success of the continuum theory for the nematic phase, particularly in relation to the visco-elastic theories introduced by Frank, Leslie, and Ericksen[3] paved the way for the extraordinary development of the wide variety of nematic-phase based LCDs.

However, the construction of a continuum theory for the more ordered, layered smectic liquid-crystal phases has been considerably less successful. Investigations of the properties of complex, and often chiral, smectic liquid-crystal systems, such as ferro-, ferri-, antiferroelectricity, pyroelectricity, and electroclinism[4–7] have led to results which suggest that the more ordered ,liquid-crystal phases, even of classical rigid-shape anisotropic mesogens, may not necessarily be homogenous systems. For example, consider the ferroelectric response of the chiral smectic C* phase of a classical rigid rod-like smectogen such as (2*S*)-methylbutyl 4′-nonanoyloxybiphenyl-4-carboxylate (**1**) to applied electric fields.[8] Any

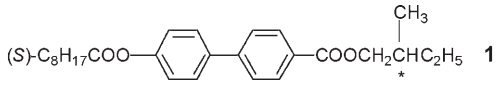

type of intrinsic (proper) ferroelectric material should, in principle, exhibit a dielectric hysteresis loop. Ferroelectric liquid crystals are essentially extrinsic (improper) ferroelectrics, with the ferroelectric properties being driven by the

Professor John W. Goodby is the Past President of the International Liquid Crystal Society. He studied for his PhD under the guidance of Professor G. W. Gray before moving to AT&T Bell Laboratories in the USA where he became Supervisor of the Liquid Crystal Materials Group. Currently he is Chair of Materials Chemistry at the University of York, UK. His research in liquid crystals has been recognized with the GW Gray Medal of the British Liquid Crystal Society, the Tilden Lectureship of the RSC, an Honorary Doctorate from Trinity College, Dublin, and the Interdisciplinary Award of the RSC.

tilting of the chiral molecules within the layers of the mesophase.[9] Hence the appearance of a macroscopic spontaneous polarization in materials such as **1** is due to the impossibility of a complete averaging of individual molecular transverse dipole moments within a layered structure that is of reduced local symmetry as a result of the chirality of the molecules (see Figure 2). The spontaneous polarization can

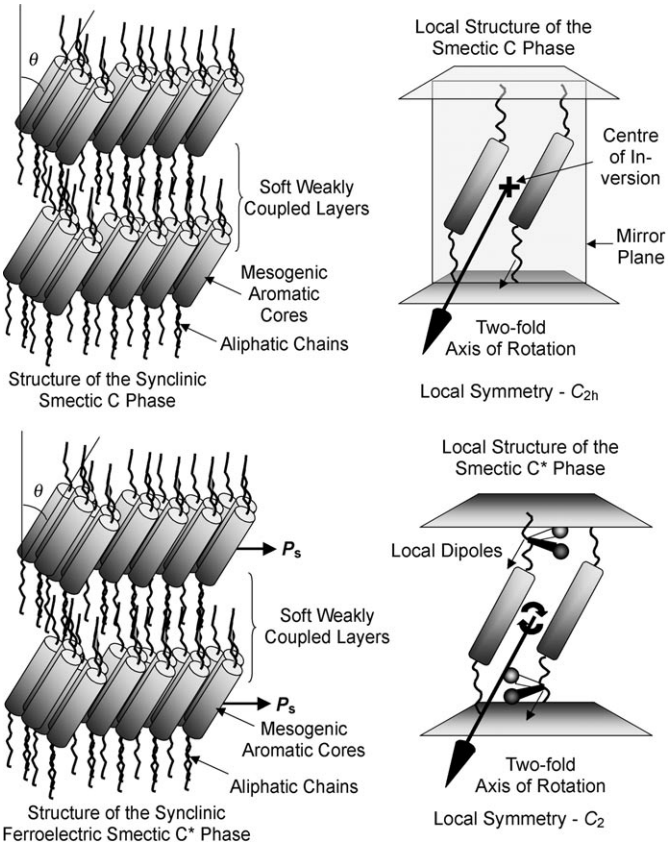

Figure 2. The local symmetry elements for the achiral smectic C phase (top), and the chiral smectic C* phase (bottom). The latter is the ferroelectric phase and is depicted with a positive spontaneous polarization ($P_s(+)$). For a negative P_s the polar C_2 axis would point backwards into the page.

be either positive (P_s+) or negative (P_s-) and the direction was shown to be related to the configuration of the stereogenic center of the material.[10]

For compound **1**, however, the direction of the spontaneous polarization was found to invert as a function of temperature (Figure 3).[11] The inversion of the direction of the spontaneous polarization could not be explained by the theories of the time, and so a new model was proposed where two conformational species, A and B, of opposite polarization directions competed with one another as a function of temperature.[11] At high temperatures species A might be expected to dominate, and at lower temperatures species B would dominate. However, in this model it was also presumed that there was an interconversion between A and B, that is, the concentrations of A and B fluctuate. The consequence of this theory was that the ferroelectric smectic C* phase was

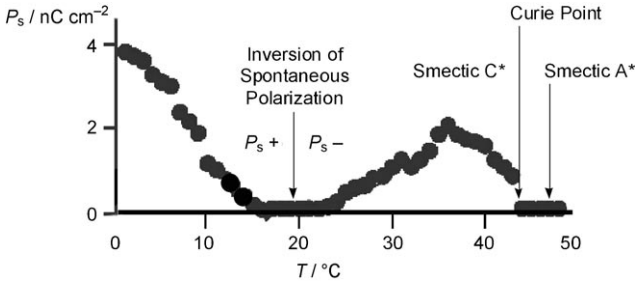

Figure 3. The spontaneous polarization for compound **1** as a function of temperature (°C).

inhomogeneous and made up of potentially rapidly fluctuating and interconverting domains. This postulation was supported further by pyroelectric studies which showed the inversion temperature was dependent on the magnitude of the applied electric field. From these studies the effective cluster size was determined, and found to be approximately (20 ± 6) Å in three dimensions.[7]

The question with respect to the nature of the fluctuating domains remains unresolved. However the energy barrier was determined for compounds such as **1**, and was found to be comparable with conformation changes between the *gauche* and *trans* conformers associated with the local structure about the stereogenic center, (Figure 4). The two conformers would engender opposite spontaneous-polarization directions owing to the associated inductive effects at the respective stereogenic centers, thereby providing a mechanism for the inversion phenomena. Thus, it was proposed that the *gauche* and *trans* conformers could act as local templates for the formation and packing of similar conformers in a time- and temperature-dependent fluctuating system. A snap-shot of the fluctuating system of A and B conformers is shown in Figure 5. In a real fluctuating system of course, more conformers and domains would be expected to be present.

Other examples of well-known phenomena in liquid-crystalline phases of classical rigid-rodlike mesogens that cannot easily be explained within the framework of the

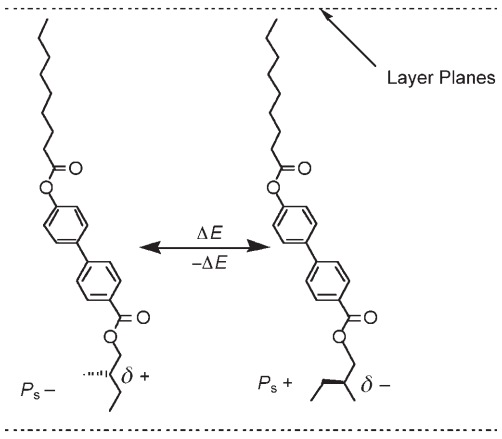

Figure 4. The *trans* and *gauche* conformers, tilted such that their aromatic cores have a higher tilt angle than the chains or the molecules alone. This type of layer organization was suggested from the X-ray studies of Bartolino et al.[12]

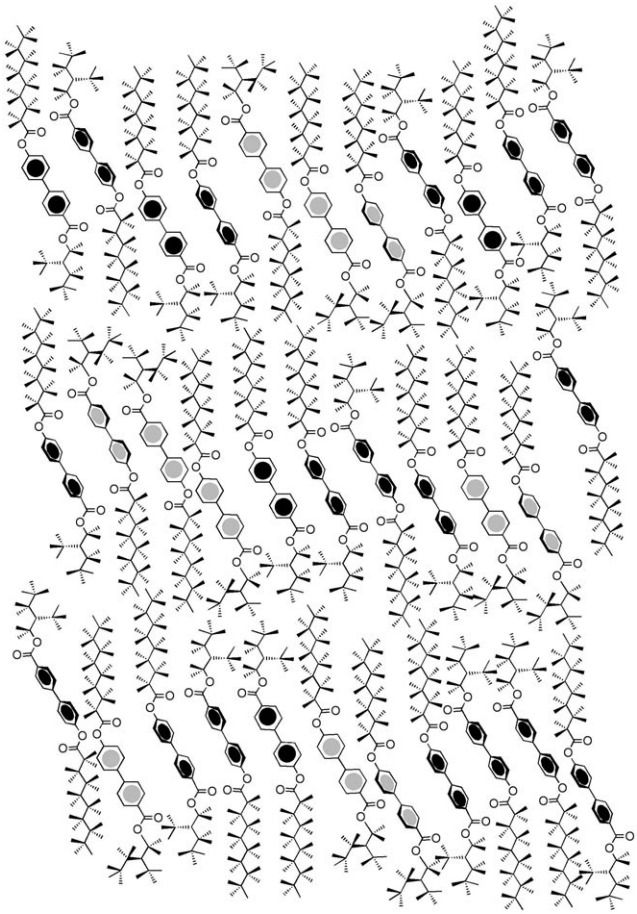

Figure 5. Fluctuating domains of confomers A and B in a ferroelectric liquid crystal.

Helix Inversion in the Cholesteric Phase

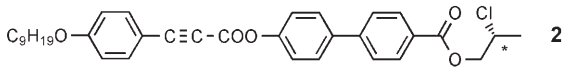

Cryst 103 SmA* 137 N^*_R 141 N^*_∞ 143 N^*_L 166 °C I

Helix Inversion in the Smectic C* Phase

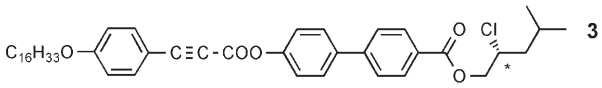

Cryst 60 SmC^*_R 43 SmC^*_∞ 49 SmC^*_L 101 SmA* 113 TGBA*114 N* 116 BP 117 °C I

Helix Inversion in the Cholesteric and SmC* Phases and P_s Inversion

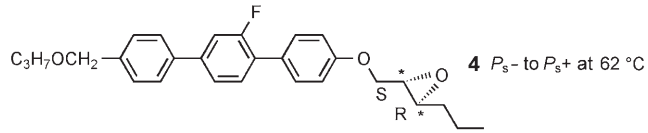

Cryst 59 SmC^*_L 46 SmC^*_∞ 47 SmC^*_R 103 N^*_L 106 N^*_∞ 112 N^*_R 159 BP 164 °C I

Helix Inversion in the Cholesteric Phase

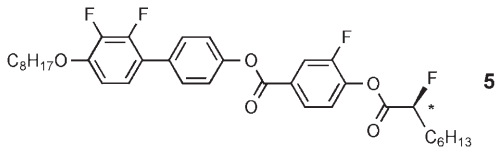

Cryst 90 SmC* 139 N^*_R 140 N^*_∞ 140 N^*_L 150 °C I

Scheme 1. Compounds showing helix inversion in one-component systems. L left-hand helix, R right-hand helix, and ∞ infinite pitch length.

continuum theory include the observation of helix inversion in the chiral smectic C* and chiral nematic phases of single-component (enantiomer) systems,[13,14] see structures **2** to **5** (scheme 1). Again, it is possible to interpret such inversion phenomena as being associated with competing species, species that try to form a left-hand helix and those that try to form a right-hand helix. The competition is driven by concentration as a function of temperature.

As mentioned above, the properties of the nematic phase of classical rigid-rodlike or disclike mesogens are usually well-described by the continuum theory. However, there are instances where fluctuating clusters of molecules have been detected in the nematic phase. These fluctuations are sometimes thought of as cybotactic groups, and are usually associated with smectic A and smectic C fluctuations within the temperature range of the nematic phase. Yet, no noticeable thermodynamic changes have been detected in association with the fluctuations.

Time-dependent clustering and domain formation have also been postulated in liquid-crystal phases of rigid-rodlike mesogens including near the transition from isotropic liquid (I) to twist grain boundary (TGB), and between blue phase (BP) and cubic D phase.[15]

Even though in the solid state, stable domain models are reasonable presumptions to make, for liquid-like systems domains would not be expected to be stable over long periods. Thus the time dependency has to be considered for domain-formation phenomena occurring in liquid crystals.

This picture of the structure of a liquid-crystalline phase as a rapidly fluctuating domain system is reminiscent of early attempts to rationalize the liquid-crystal state in which models were developed based on molecular interactions. The resulting hypothesis was called the "swarm theory" of liquid crystals. The swarm theory interprets the liquid-crystalline state as a consequence of intermolecular interactions within the context of statistical thermodynamic equilibria. Thus, for the swarm theory the molecular interactions form the basis of the theory whereas for the continuum theory, the molecular interpretation of the macroscopic parameters is more or less given up, but it is by no means totally suppressed.[16]

The swarm theory originally proposed by Bose, and until the 1960s used as a basis for the interpretation of experimental results, was elaborated on by Ornstein et al.[17] Bose's hypothesis assumed that liquid-crystal phases were composed of swarms of molecules which were in more or less parallel orientation, and that these anisotropic swarms were in vigorous thermal dynamic motion so that the mass as a whole would be isotropic. He theorized that the swarms had to be of colloidal dimensions, with a diameter less than the wavelength of light. Bose's concept has the surprising result that the forces between molecules within the small swarms are able to produce a rather high degree of order and, con-

sequently, a high birefringence, whereas the forces between swarms are so weak that the mass as a whole is isotropic and completely disordered.

However, questions were raised over the validity of the swarm theory, these included: could systems composed of swarms be considered as phases according to thermodynamics; be capable of exhibiting a sharply defined mesophase surface at the transition to the isotropic liquid; and be characterized by sharp transition temperatures from one mesophase to the next?

According to Gibbs, a phase is a homogeneous system in thermodynamic equilibrium, whether it is made up of atoms, molecules, or colloidal particles. Thus the principle of homogeneity depends on the size of the elements from which the system is constructed and the observation level. In the context of larger elements, Zocher et al. demonstrated it was possible for certain phases, usually lyotropic phases, to be composed of colloidal- or nanoparticles to yield phases they described as "phases of higher order" or "superphases".[18]

In recent years the chemical structures of liquid-crystalline materials have often deviated radically from the classical design principles bequeathed from Reinitzer's days, where rigid rodlike or disclike mesogens were used in the attempt to create liquid-crystal phases. Indeed, the discovery that bent molecular systems exhibit whole new families of mesophases has led to the investigation of the liquid-crystal properties of materials with widely varying molecular topologies and sizes—from pyramids to crosses to larger dendritic molecules.[19]

Herein we seek to give evidence of some of the unusual behavior encountered in mesophases formed by nonconventional molecular topologies. Owing to unusual shapes, interactions, topologies, or sizes in these systems, the templating and the formation of fluctuating domains or clusters can occur because of restricted motions. We describe observations, such as 1) mesophase stabilization through conformational change in systems with deformable molecular shapes, 2) topologies of supermolecular and self-assembled supramolecular systems, 3) surface recognition processes of superstructures, 4) end-group-mediated transmission of information across layer interfaces, and 5) the amplification of information within mesophases.

All these phenomena imply that the length scales that are normally used to describe liquid crystals are not necessarily valid. It is the unusual nature, strength, and combination of molecular interactions in these novel systems that lead to a breaking of apparent homogeneity on an observable level. It thus seems that liquid-crystalline systems need to be considered as fluctuating and dynamically changing, multihierarchical fluids, with molecular interactions manifesting themselves in localized supra- and super-structures through processes of self-assembly and self-organization (Figure 6).

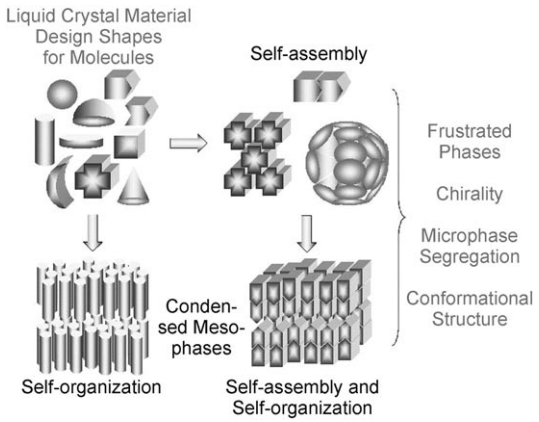

Figure 6. The structures formed by self-organizing and self-assembling liquid crystals.

2. Topology and Shape Deformation in Supermolecular Systems

In the early design of small molecular systems for the exhibition of liquid-crystal phases, the shapes of the molecules were characterized as either rods, discs, or spheres. To accommodate lyotropic systems, amphiphiles were included as a separate category. For the most part, the study of small molecular systems dominated the field because of the close link between molecular design and commercial applications. However, it is only in the last twenty years that materials with unusual, and often hybrid structures have been investigated for their liquid-crystalline behavior. Most notably phasmidic materials, which have molecular structures that are part-disc part-rod, were found to exhibit both columnar and smectic phases. More recently, molecular systems having bent structures have been investigated and found to exhibit a wide range of novel phases, many of which were found to be ferroelectric or antiferroelectric (without molecular chirality) owing to the reduced symmetry of their mesophase structures.

In the area of super- and supramolecular liquid crystals, many different expressions have been used to describe some of the same structures, and for more complex structures this has led to some confusion. Figure 7 shows some typical molecular architectures which can be used to describe the structures of supermolecular liquid crystals. For example, two mesogenic units, that is, molecular entities that favor mesophase formation, can be bound end-to-end (terminally) to give linear supermolecular materials. If the mesogenic groups are the same they are called dimers, but if they are different they are referred to as dimesogens. The mesogenic units may also be linked together laterally, rather than terminally, or they may have terminal units linked to lateral units to give T-shaped dimers or T-shaped dimesogens. With trimesogens the situation becomes more complicated because not only are there linearly and laterally linked possibilities for the supermolecular structures, but also there are structures where the mesogenic units could be linked to a central point, creating a "molecular knot". In a similar way, tetra-, penta-, and higher mesogen supermolecules can be created. Increased numbers of mesogenic units attached to a central point can be created by introducing a central scaffold upon which to add the mesogens to create the supermolecular structure. Thus cyclic, caged, or hyperbranched scaffolds, with inbuilt hierarchical structures, can be utilized. The possibilities for supermolecular structural design then become endless.[20]

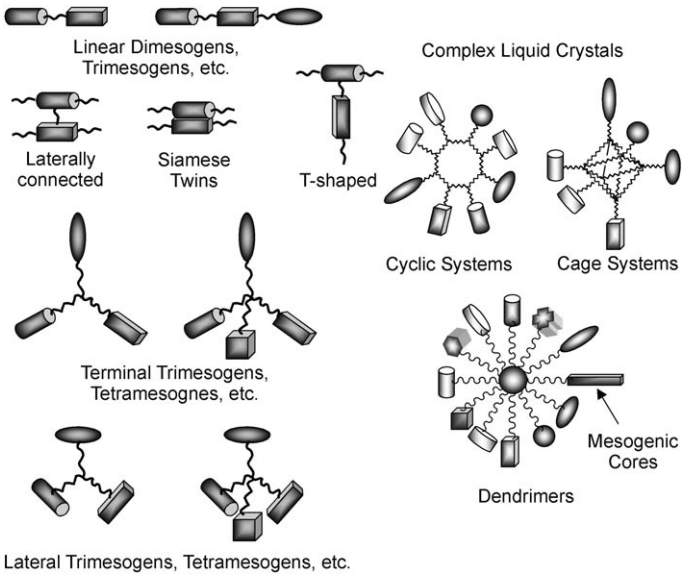

Figure 7. Templates for the design of liquid-crystalline supermolecular materials. The mesogenic units are shown as differing shapes, however, the materials may be constructed with mesogenic units of the same type (homosystems).

If we focus on liquid crystals built onto scaffold structures, then the supermolecular materials can be thought of as dendritic structures when the mesogenic units are all of the same type. Figure 8 depicts the general structure of a

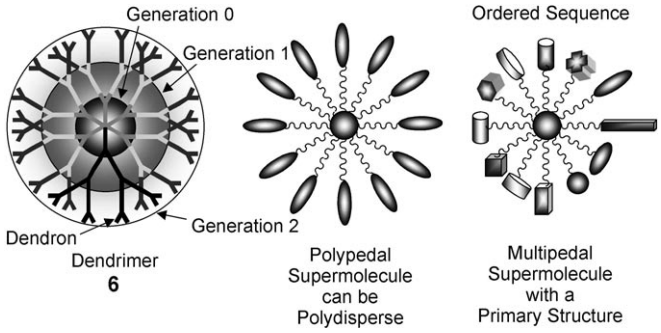

Figure 8. A dendritic scaffold **6**, a polypedal, and a multipedal supermolecule.

dendrimer **6** where repeating branched hierarchical units are linked together one shell on top of another to create various generations of the dendrimer. If identical mesogenic units are located at the surface of the dendritic scaffold, then a dendritic liquid crystal, or a polypedal (an object having many "feet" which are the same) supermolecule is created. Alternatively, if the mesogenic units are mostly different with respect to one another, then the supermolecule will have many different feet, and thus could be termed a multipedal supermolecule. There is a clear distinction between these two types of supermolecular system; the polypedal supermolecule, like a polymer, is subject to polydispersity, whereas the multipedal supermolecular material is not; it has a defined primary structure, like a protein. In fact Newkome et al. make the observation that "*on the preparation of dendritic macromolecules, the continued inability to ascertain the absolute homogeneity of the resultant structures has led many to claim the monodisperse character of their products*".[21]

2.1. The Self-Organization Processes

The way in which supermolecules can self-organize is dependent to a large degree on simple structural features, such as the density of the mesogenic units attached to the periphery of the central scaffold, their orientation of attachment, and the degree to which they are decoupled from the scaffold (Figure 9). For example, the density of mesogenic

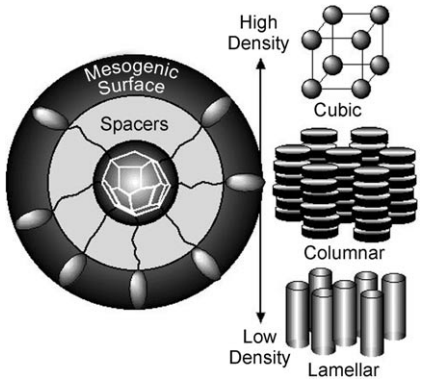

Figure 9. Effect of the number density of mesogens on the surface of the supermolecular structure on the formation of various mesophases.

groups attached to the periphery can effectively change the topology of the structure of the supermolecule from being rodlike, to disclike, to spherulitic.

The scaffold, of course, can be varied while the same type of mesogenic unit is retained. Scheme 2 shows a systematic study where (*S*)-4″-(oct-2-yloxy)-2,3-difluoroterphenyl mesogenic units (**X**) are retained but the scaffold is varied (**7**–**12**). From dimers to trimers to tetramers, all of the supermolecules exhibit smectic C* phases. It is only when the octamer **12** is reached that a smectic A* phase appears. However, these results clearly show that smectic polymorphism is possible within the system of rodlike topologies. It is also interesting that the smectic C* to isotropic liquid or the smectic A* transition is similar across the whole family of materials, given their sizes, except for **7**, suggesting that the liquid-crystal properties are being controlled by the mesogenic group and that the scaffold does not play a major part in mesophase formation. Thus deformability occurs most easily away from the scaffold even though the linking chain between the mesogenic units and the scaffolds is relatively short (five CH_2 groups).

Although the structures of supermolecules at a molecular level can be considered as being deformable, it is also possible for a given type of molecular architecture to change its shape depending on the external conditions, such as temperature and pressure, and hence support different types of self-organized mesophase structures and mesophase sequences.

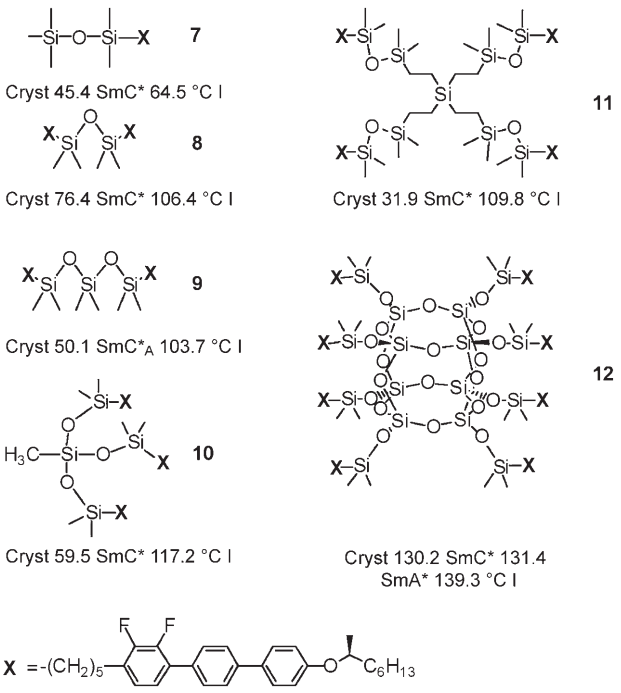

Scheme 2. Effect on the liquid-crystalline properties of a systematic variation of the type of scaffold for a constant mesogenic unit **X**.[22]

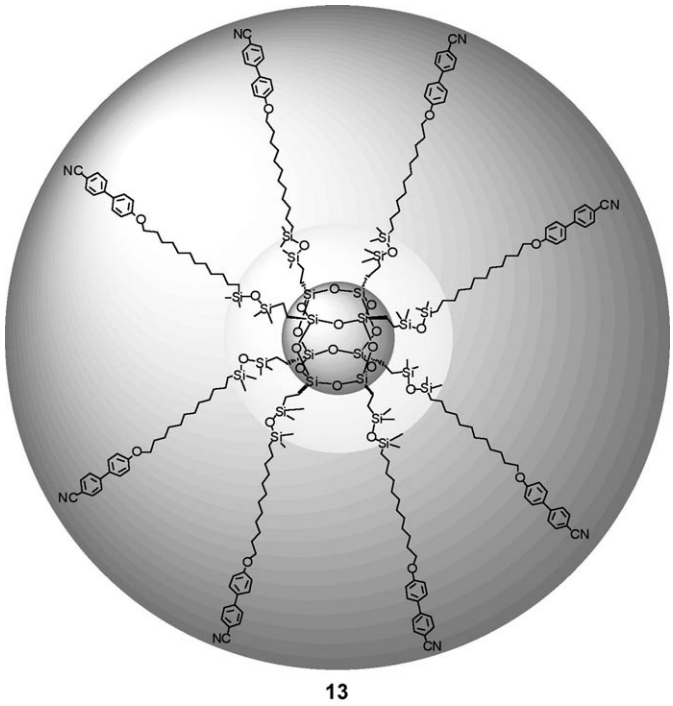

2.2. Orientation of Mesogen Attachment

Although there have not been extensive research studies into the effects that the type (rod, disc, or spherulitic) of mesogenic group attached to the central scaffold has on mesophase formation, it is well documented for rod-shaped mesogenic groups that the orientation of the attachment can markedly influence the type of mesophase found and the polymorphism of any smectic phases formed. As with side-chain liquid-crystal polymers (SCLCPs), lateral attachment (side-on) of the mesogenic units often leads to supermolecular systems exhibiting nematic phases, whereas for terminal attachment (end-on) smectic phases appear to predominate.

In the first example we discuss, the scaffold structure is maintained throughout the study and the mesogens are terminally attached. Supermolecule **13** is an octamer based on the octasilsesquioxane core unit.[23] This material was prepared and purified in such a way that by HPLC and ^{29}Si NMR spectroscopy it was shown to be a single compound without dispersity. This material, like the silsesquioxane derivative **12** (Scheme 2) exhibits smectic polymorphism with a smectic C and a smectic A phase being formed. The incorporation of cyanobiphenyl mesogenic moieties means that the material has interesting dielectric properties, and the presence of the smectic C phase indicates that with the introduction of chirality, the material would also be ferroelectric and pyroelectric. The mesophase sequence of SmC-SmA-I demonstrates that the dendritic structure of the supermolecule is constrained to being rodlike, and the rodlike conformers tilt over at the smectic A to smectic C phase transition (Figure 10). Thus, the structures of both the smectic A and the smectic C phases have alternating organic and inorganic layers. As the inorganic and organic layers have differing refractive indices, the mesophase structures are essentially nanostructured birefringent slabs.

The number of mesogenic groups can be increased in the periphery to sixteen. The resulting polypede **14** shows a phase sequence of g –17.5 SmC 63.1 SmA 91.7 °C I (g: glassy). Thus the effective doubling of the number of mesogenic units has the effect of lowering the clearing point, the SmA to SmC transition, and the glass transition relative to **13** (g –12.8 $Cryst_1$ 4.7 $Cryst_2$ 39.0 SmC 74.2 SmA 102.9 °C I). This thermal behavior is in contrast with that normally found for liquid-crystal dendrimers based on flexible dendritic cores, where the clearing points increase and the glass transitions remain almost constant with generation number.[24]

The mesophase behavior of **14** implies that the dendrimer must have a rodlike shape so that it can pack in layers, in which the molecules within the layers are disordered and the

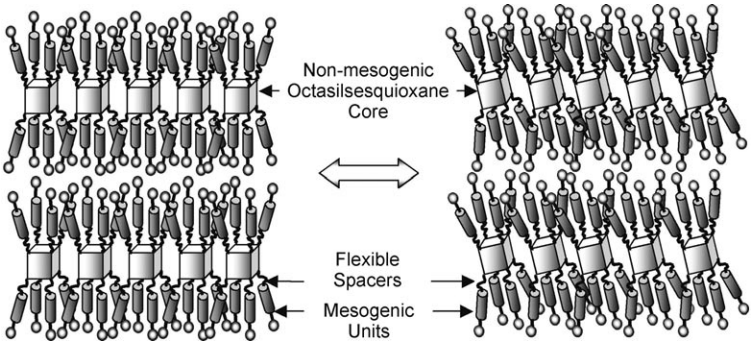

Figure 10. Schematic drawing of the bilayer structure of the smectic A (left) and smectic C phases (right) of supermolecule **13**. The eight mesogenic units per molecule are accommodated in the layers without the introduction of curvature in the packing of the mesogenic units.

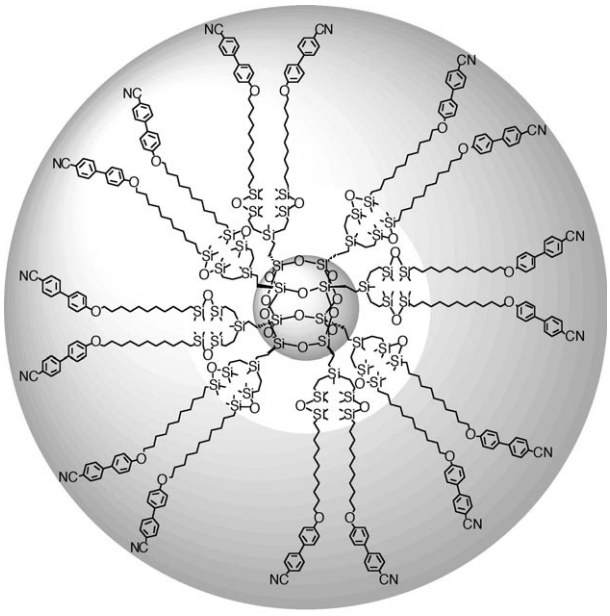

14

M_w / M_n = 1.06; coverage (by NMR): 14 ± 2 mesogens per molecule

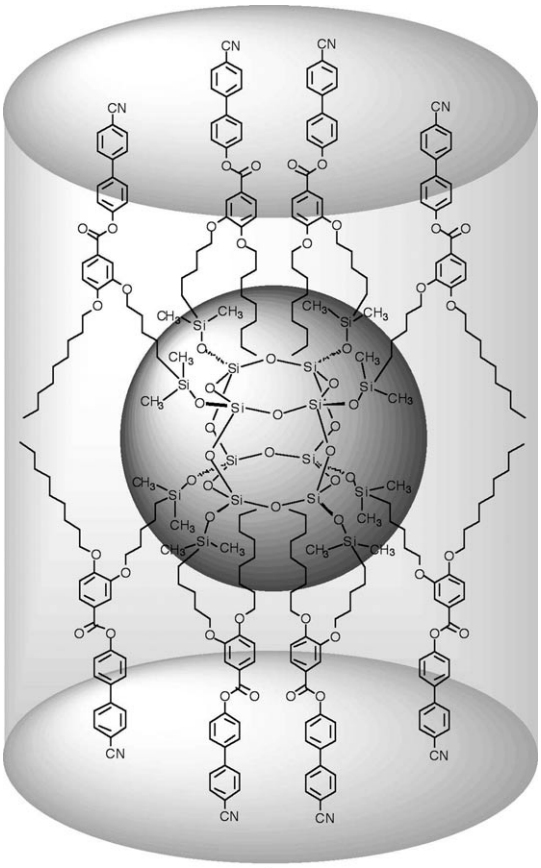

15

layer structure is diffuse, revealing that the mesogenic state deforms the globular environment of the dendrimer. This situation is remarkable given that the number of mesogenic units is doubled relative to the number of octasilsesquioxane scaffolds, and where as a consequence a curvature in the packing of the mesogenic units would be expected to occur as a result of their bunching about the scaffolds.

Comparing the results obtained on the liquid-crystal properties for the terminally appended supermolecule with those obtained for the laterally appended supermolecule **15**, we find that the side-on mesogenic subunits lead to the formation of an enantiotropic nematic phase, albeit with a small temperature range (g −25 Cryst 48.9 N 51.8 °C I).[25] Thus it is clear that it is possible to control the type of mesophase formed through the nature of the attachment of the mesogenic group to the scaffold.

Given that lateral appending mesogenic groups can lead to the formation of nematic phases, then by laterally appending chiral mesogenic units to the octasilsesquioxane scaffold the chiral nematic phase can be introduced into this class of materials. The fourth supermolecular material **16** demonstrates this effect. The material has the size of a small globular protein, and as expected, it exhibited a chiral nematic phase with a helical macrostructure. The material exhibits an extraordinarily long temperature range for the chiral nematic phase. A transition from a glassy state to the chiral nematic phase occurs near to room temperature and then the phase extends over ninety degrees before transforming to the isotropic liquid at 116.9 °C.[26] The local structure of the chiral nematic phase is shown in Figure 11 (left) where the supermolecules **16** are shown as having rodlike or tubular structures and the mesogenic units are expected to intermingle between the supermolecules. The

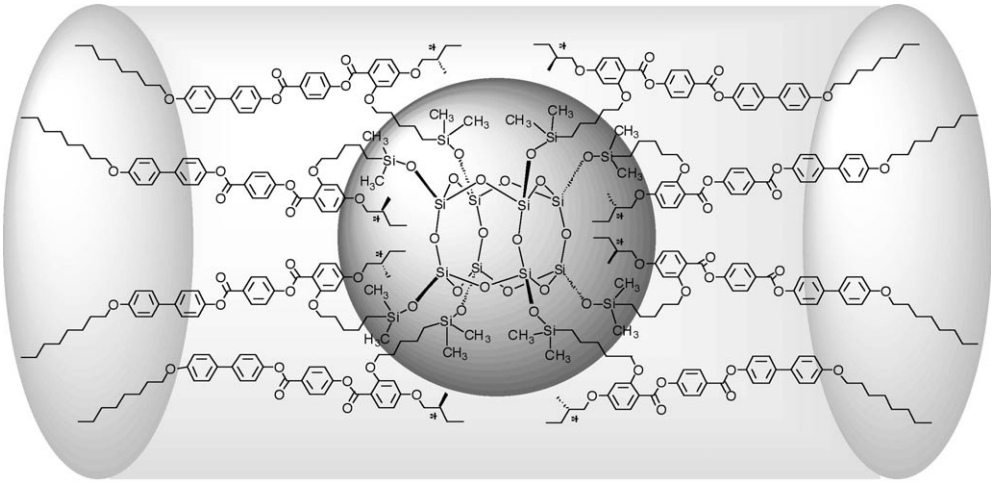

16

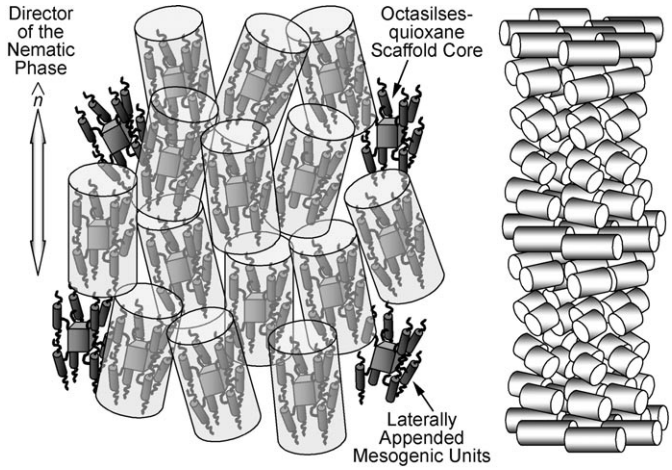

Figure 11. The local nematic structure (left) and the helical macrostructure (right) of the chiral nematic phase of dendrimer **16**.

chiral nematic phase will have a helical macrostructure superimposed upon the local nematic ordering (Figure 11; right).

Remarkably the supermolecular compound **16** has a helical pitch of approximately 2 μm, which is a relatively short pitch considering its molecular dimensions, and it is approximately the same as the pitch that would be produced by the individual mesogenic units without lateral chains being attached. However, unlike for the individual mesogenic species, the pitch is relatively temperature insensitive. Thus the surface of the supermolecule acts as a molecular recognition surface, in a similar way as recognition surfaces are created in surfactant systems and Janus grains as described by de Gennes.[27]

By changing the point of attachment of the mesogenic groups and through the introduction of stereogenic centers, it can be shown that through molecular deformation into overall rodlike structures, supermolecular materials can exhibit polymorphism and helical macrostructures. Increasing the density of the mesogens through bifurcation of the scaffold, so that twice the number of mesogenic units can be bound to the central scaffold, allows the effect of change in molecular shape to be investigated. Thus, supermolecular material **17**, which has sixteen side-on attached mesogenic units, was prepared. Upon heating and cooling chiral nematic, hexagonal disordered columnar, and rectangular disordered columnar phases were observed (g 5.4 Col^*_{rd} 30 Col^*_{hd} 102.3 N* 107.7 °C I).[28] Thus the increase in the density of the mesogens bound to the central scaffold in going from octamer **16** to hexadecamer **17**, results in a transformation from calamitic phases to columnar phases. However, the formation of columnar phases when the dendrimer has rodlike mesogenic groups is not easy to explain unless the mesogenic groups surround the octasilsesquioxane core to give a short cylindrical structure.

From the point of view of the mesophase structure, the best fit to the X-ray data of **17** was obtained using such a

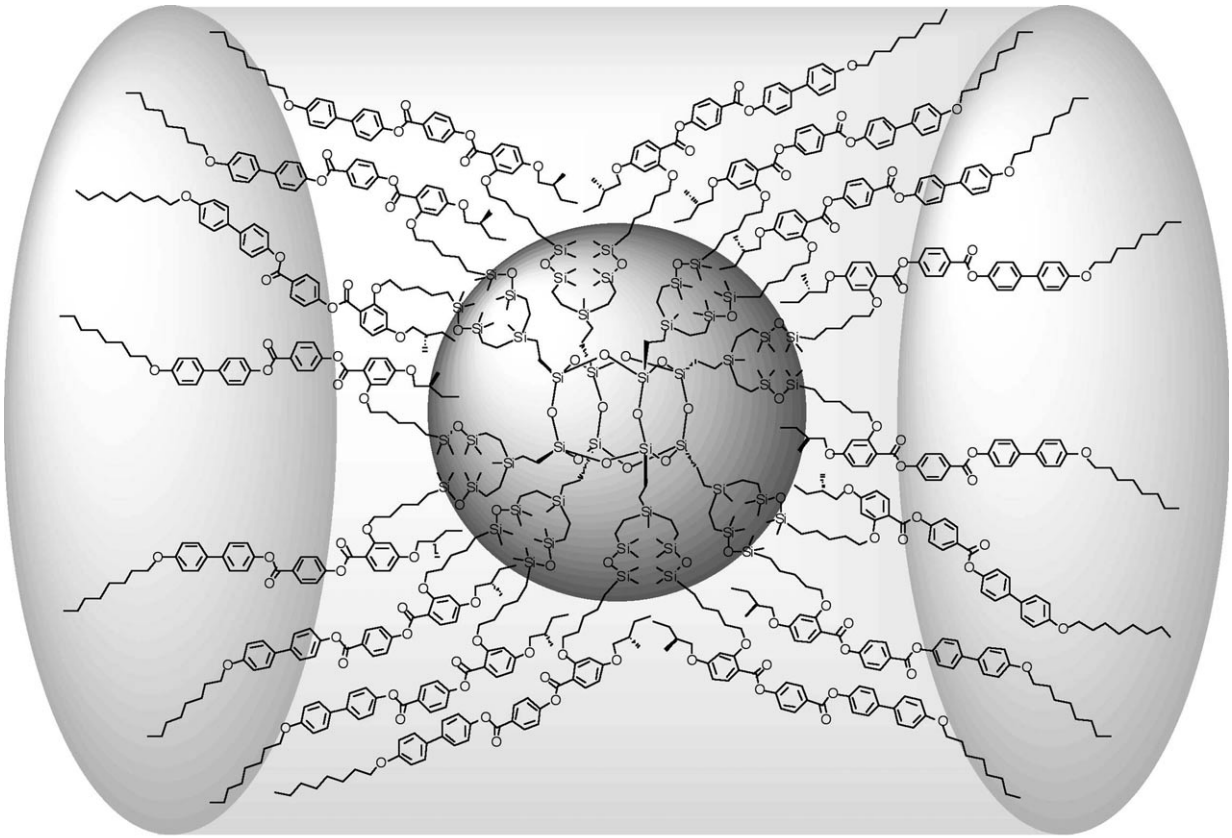

17

model, which suggests that in the hexagonal columnar phase the dendrimer assumes a cylindrical shape that has approximately the same height as its diameter. The long axes of the mesogenic units are roughly parallel to, or slightly tilted with respect to, the rotational axis that is normal to the cylinder, that is, the mesogenic units are nematic-like, and they are packed together side by side on the outer surface of the cylinder. These remarkable new mesophase structures, which are essentially variations of "tubular nematic-columnar phases", are favored by the spacer length of five methylene units used to attach the mesogen to the dendrimer core. The short spacer length prevents full decoupling of the mesogenic motions from the silsesquioxane cage forcing the mesogens to pack closely together around the dendritic core. The structures of the "hexagonal tubular or nematic-columnar" and "rectangular tubular or nematic-columnar" phases are shown schematically together in Figure 12.

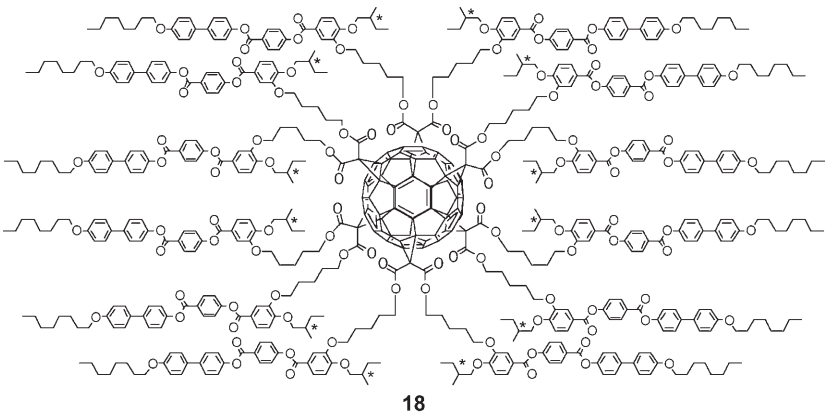

18

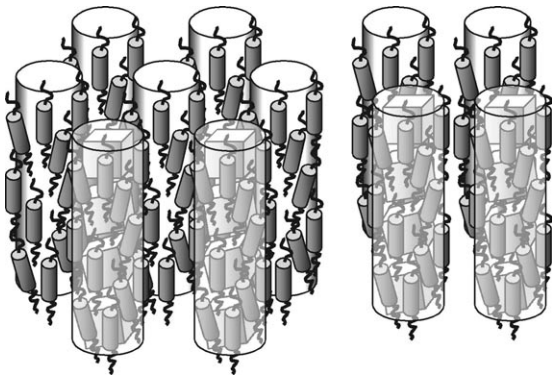

Figure 12. The hexagonal (left) and rectangular columnar phases (right).

The hybrid structures of these novel liquid-crystal phases are potential model systems for the development of photonic band-gap materials, where large differences in refractive indices between the inorganic and organic sections can be engineered into the system through material design and self-organization. Furthermore, the hexadecamer **17** has a pitch in the chiral nematic phase of approximately 0.3 to 0.4 μm, and thus exhibits the selective reflection of blue light.

2.3. Nanomolecular "Boojum"

Apart from employing octasilsesquioxane as the central scaffold other rigid cage structures can be used as the central building block. For example, supermolecular material **18** has a structure that utilizes the same laterally appended mesogens as in **17**, but this time they are attached to a [60]fullerene (C_{60}) central core unit.[29] Through bifurcation twelve mesogenic units were symmetrically positioned about the C_{60} core, thereby creating a spherical architecture. Again, because of the lateral attachment of the mesogenic units, a chiral nematic phase is exhibited by this material. The material forms a glass at 47 °C, and upon heating a chiral nematic phase is stable up to 103 °C.

The mesophase defect textures exhibited by **18** were typical of those normally found for a chiral nematic phase, except they were only revealed upon annealing, which is probably a result of the viscosity of the material. Thus the sample was annealed just below the clearing point. After 24 h, large areas of the preparation evolved to show fingerprint defects and the Grandjean plane texture (see Figure 13). From the Grandjean plane texture the twist sense of the helical structure was found to be left-handed. The pitch was determined by measuring the number of pitch bands per unit length from the fingerprint texture. A value of 2.0 μm for the pitch length was obtained at room temperature. The value was found to be similar to those of the chiral mesogen unit (1.7 μm) and the malonate precursor (1.9 μm). Thus the fullerene moiety is shielded very effectively by the laterally attached mesogens, without disturbing the helical supramolecular organization of the mesophase. Furthermore, as the mesogenic units are symmetrically distributed all over the fullerene sphere they effectively isolate it, thereby decreasing the possibility of aggregation of the C_{60} units, which is detrimental to mesophase formation.

It is also interesting to consider how the selection process for the helical organization of material **18** is generated upon cooling from the isotropic liquid. As the C_{60} core of the material is spherical, and the mesogenic units are attached by relatively short methylene spacer units, it is not unreasonable to assume that, in the liquid phase, the mesogenic units are symmetrically disposed about the central core. Cooling into the chiral nematic phase, however, the helical organization would be expected to be a result of the organized packing of the dendritic supermolecules, that is, they are considered to be no longer spherical in shape. However, it was found that when the diameter of the C_{60} core is compared to the length of the mesogenic units, it is clear that flexible, random packing of the mesogenic units about the core in the liquid-crystal state is not possible, and that the mesogens are required to be organized in their packing arrangements relative to one another, both on the surface of the dendrimer and between individual dendrimer molecules. One possibility was postulated where the

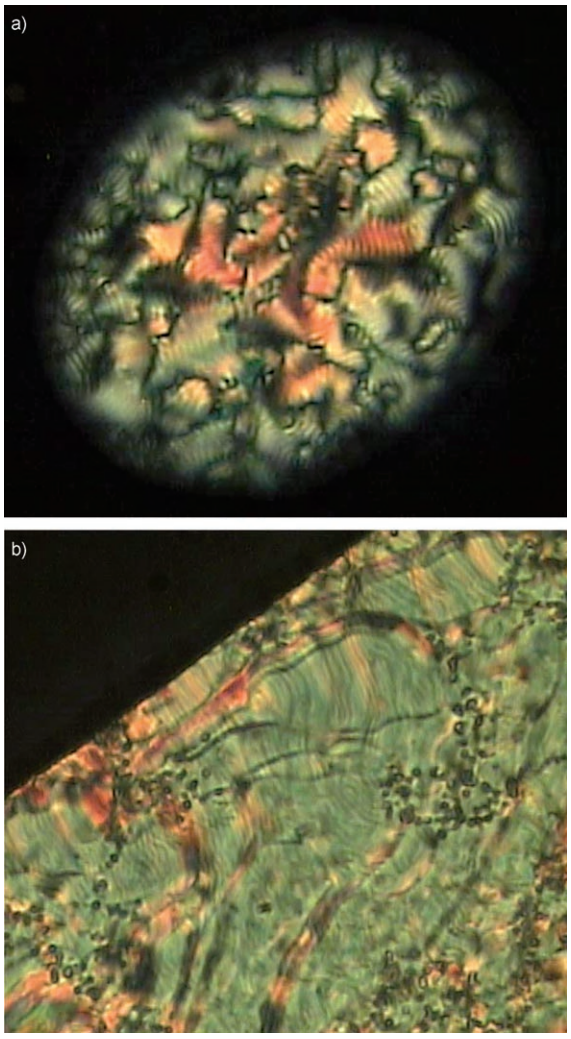

Figure 13. a) Fingerprint texture for an uncovered droplet of compound **18**, and b) the Grandjean texture of the chiral nematic phase.

mesogenic units are oriented parallel to one another, thus when the material cools into the liquid-crystalline phase directional order of the mesogens is selected by the external environment, such as the surface. This information is then transmitted to the other mesogens associated with the spherical dendrimer and further to the neighboring dendritic supermolecular compounds.

Alternatively, for an individual dendrimer it was proposed that the direction of the mesogens would spiral around the C_{60} core to give poles at the top and bottom of the structure, as shown in Figure 14. Thus the spherical dendrimer was projected to have a well-defined chiral surface, thereby resulting in the creation of a chiral nanoparticle, that is, a nanomolecular "Boojum". When the chiral nanoparticles pack together they were expected to do so through chiral surface recognition processes, resulting in the formation of a helical supramolecular structure. Consequently, the chiral supermolecular nanoparticles transmit their local organization through amplification to adjacent molecules which results in a helical twisting power that is higher and a pitch

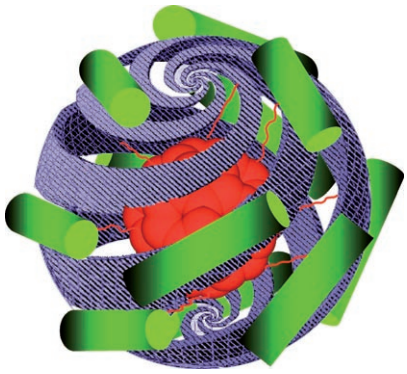

Figure 14. Proposed helical structure of a nanomolecular "Boojum".

that is shorter than might be expected for such large molecular entities.

2.4. Janus Liquid Crystals

As seen from the potential to form "Boojum" nanostructures (Section 2.3), one of the more intriguing aspects in the self-organization of complex fluids is understanding the manner of molecular recognition processes in materials with diversely functionalized faces or sides. Such supramolecular objects may recognize and select left from right, or top from bottom, as described by de Gennes.[27] In this respect a new concept was devised for the design of self-assembling functional liquid crystals[30] called "Janus" liquid-crystalline molecular materials (Figure 15). These materials take the

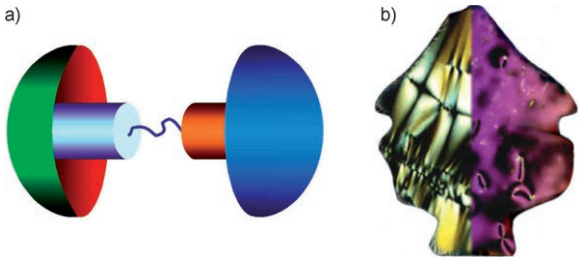

Figure 15. a) Design of Janus liquid crystals; two hemispheres possessing differing liquid-crystal types which alone would form different mesophases, b) two-faced system composed of smectogenic and nematogenic materials.

form of segmented structures that contain two different types of mesogenic units, which can favor different types of mesophase structure, grafted onto the same scaffold, to create giant molecules that contain different hemispheres "Janus" refers to materials with two faces, such as fluorocarbon/hydrocarbon or hydrophilic/hydrophobic. For example, a Janus supermolecule with hydroxy and hydrocarbon faces has been recently reported[31]. Thus, the complementary materials **19** and **20**, based on a central scaffold made up of pentaerythritol and amino[tris(hydroxymethyl)]methane units linked together were studied, where one unit carries three cyanobiphenyl (CB; smectic preferring) and the other three chiral

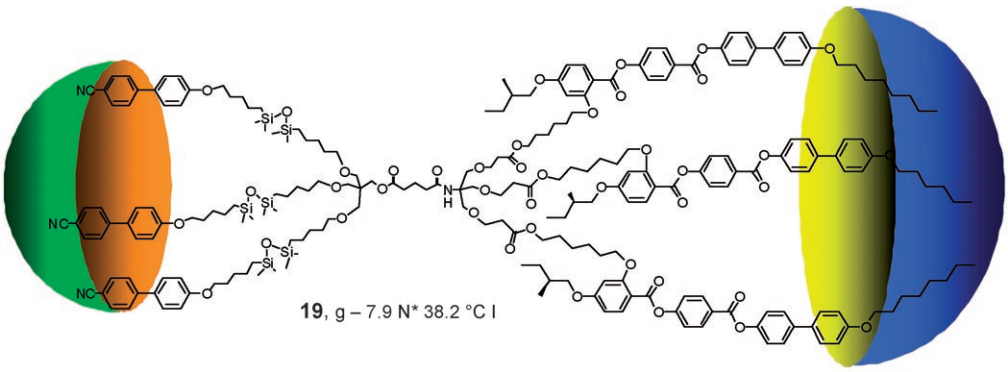

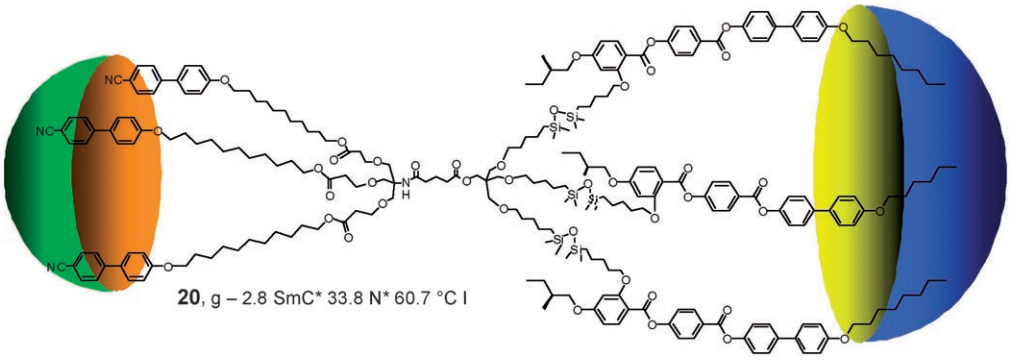

phenyl benzoate (PB; chiral-nematic preferring) mesogenic moieties or vice-versa.[32]

The Janus supermolecular material **19** exhibits only one enantiotropic transition which occurs between a chiral nematic phase and the isotropic liquid, in the form of a weak and broad peak at 38.2 °C in the calorimetry trace. The only other thermal event present was a glass transition at −7.9 °C. Only when the sample was left standing at room temperature for three weeks did the material crystallize fully. Conversely, on heating **20**, a broad melting endotherm with onset at 33.8 °C was followed by a transition from the liquid-crystal state to the isotropic liquid at 60.7 °C. The cooling cycle from the isotropic liquid showed a broad, weak exotherm, onset at 60.3 °C, marking the transition to the chiral nematic phase. A second exotherm occurred on cooling, onset 36.1 °C, marking a second-order transition to a chiral smectic C* phase. Further cooling induced a glass transition at approximately −2.8 °C. It is also important to note that the formation of chiral mesophases by the two materials means that the chiral nematic phase is thermochromic and the smectic C* phase is ferroelectric and pyroelectric and will exhibit piezoelectric properties.

Comparison of the phase behavior of **19** and **20** shows that the overall topology of the molecule in respect to the inner core plays a significant role in determining the type(s) of mesophase(s) formed, since in both cases the number of mesogens of each type and the core are the same and simply inverting the central scaffold relative to the hemispheres changes the mesophase(s) observed. The manipulation of the structural fragments (mesogenic units, central scaffold, and linking units) in the molecular design of "Janus" systems allows selection of mesophase type and therefore of the physical properties and potential applications of materials. Thus the molecular design of these systems is flexible and potentially capable of incorporating functional units, thereby providing tentative steps towards the molecular and functional complexity found in living systems.

2.5. Functional Supermolecules

The concept of creating functional materials by incorporating a certain functionality within a mesogen molecule, through covalent attachment, is a bottom-up approach to self-organizing functional materials. The following examples demonstrate the incorporation of [60]fullerene as the functional unit into self-organizing supermolecular systems. Fullerene is selected as a functional unit in this case rather than a scaffold for a dendritic material. As a functional moiety it has interesting physical properties, but it is an unlikely candidate to exhibit mesogenic properties and thus it is interesting to see if such a large non-mesogenic unit can be incorporated into a mesogenic supermolecular material without affecting the mesomorphic properties. It would be interesting to apply this approach to self-organization to other functional groups which are not well adapted to being organized in nanoscale architectures.

Fullerene supermolecular material **21** exhibits an enantiotropic chiral nematic phase, with a phase sequence of g 28.2 N* 63.6 °C I. The value of the pitch of the helix of the chiral nematic phase indicated that C_{60} fits within the helical structure formed by the mesogens without causing any significant perturbation to the structure. This result, in turn, implies that although the large C_{60} unit disturbs the mesogenic interactions, therefore lowering the clearing point relative to the parent mesogenic systems, it can be effectively camouflaged within the self-organizing chiral-nematic medium, provided that enough mesogenic sub-units are available.[33]

When the number density of the mesogenic units is increased, reducing the weight fraction of fullerene units in the supermolecular structure, as in **22**, the liquid-crystal phases become more stable (compare **21** with **22** (g 24.3 N* 80.6 I)), and the spherical fullerene unit is increasingly hidden within the liquid-crystal matrix (Figure 16).[33] This result indicates that the mesogenic units have the ability to incorporate and organize non-mesogenic functional units into the self-organizing state, without too much detriment to the liquid crystallinity.

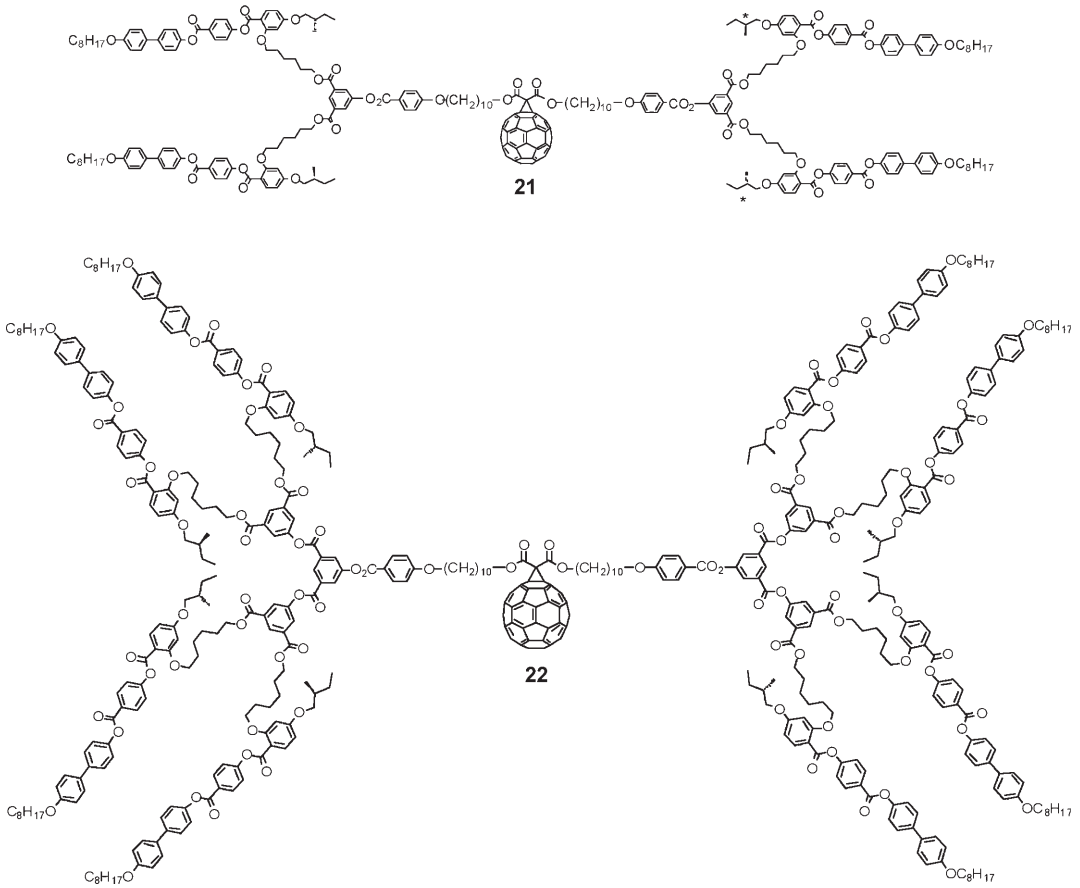

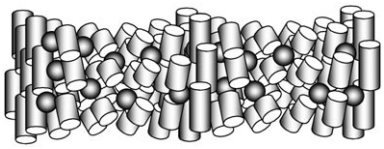

Figure 16. Helical macrostructure of a supermolecular material possessing mesogenic groups (rods) and fullerenes (spheres).[33]

2.6. Nanoparticles

The elastic distortion on liquid crystals caused by colloidal nanoparticles can result in long-range interparticle interactions that can be tuned depending on particle size, elastic properties of the liquid-crystal solvent, and the interaction between the mesogen molecules and the surface of the particles. It has been demonstrated, mainly in the nematic phase, that the anisotropic medium is able to orient and order particles, resulting in the formation of chains, particle aggregates, gels, two-dimensional ordered arrays, and soft solids, as a result of a variety of induced topological defects. This approach was proposed for magnetic particles by de Gennes and Brochard,[34] and the early studies of Cladis et al. on the mapping of the director field of the cholesteric phase showed that nanoparticles could be aligned along the local director orientation.[35]

The topological defects caused by spherical nanoparticles in liquid crystals have been extensively studied[36–42] and the predictions of Saturn rings, Boojum, surface ring, and hyperbolic hedgehog defects have been observed experimentally. These include emulsions of water microdroplets,[43–47] silicon oil,[48] silica particles,[49] and magnetic particles in a nematic host,[44,50] of silica particles in cholesteric liquid crystals,[51] of latex particles in lyotropic liquid crystals,[52] and of silica particles[53] and nanocrystals of ZnS[54,55] in the mesophases of rodlike viruses. Two-dimensional ordered arrays have been produced by the ordering of silica particles with different surface treatments[56] and soft cellular solids derived from phase separation of polymethylmethacrylate (PMMA) particles in a nematic-phase suspension.[57] In these cases the particle inclusions are in the micron size regime, and are thus much bigger than the liquid-crystal molecules. The interactions are therefore best described as being elasticity induced. When the particles are either much smaller than the liquid-crystal molecules, such as in the mesophases of viruses, or of the same order, the self-assembly is best described in terms of hard core particles, and is dominated by the entropic gain.

Metal nanoparticle assembly has been induced by several methods, among them most successful being the use of block copolymer morphologies,[58] DNA binding,[59] and viruses.[54,55] Although still in its infancy, using liquid crystals as an organizing medium to induce the assembly of metal nanoparticles is a very powerful tool because a great variety of mesophase morphologies can be achieved to control the structuring in one or more dimensions.

Gold nanoparticles coated with a monolayer of mesogenic stabilizing, calamitic[60] or discotic[61] ligands have been described. Gold nanoparticles coated with alkane-thiolates and non-mesogenic chiral aromatic units doped in a liquid-crystal solvent have been shown to form periodic striped patterns, ascribed to the accumulation of particles in chain-like aggregates.[62a] Cubic mesophases have been observed in gold nanoparticles coated with non-mesogenic dendrons.[62b] Silver, palladium, and gold nanoparticles have been doped in 4-pentyl-4′-cyanobiphenyl and the resulting mesophase shown to exhibit frequency modulation and fast electrooptic responses.[63] Platinum nanoparticles coated with surfactants dispersed in a cholesteric phase produce long-range ordered nanoparticle assemblies that mimic the helical configuration of the cholesteric liquid, however the particles do not just merely decorate the disclination lines, but generate a new helical structure of longer pitch.[64]

Titania nanoparticles of various morphologies coated with mesogenic amines[65] and α-Fe_2O_3 spindles coated with mesogenic phosphates display nematic and cubic phases when dispersed in liquid-crystal solvents.[66]

We have prepared a range of gold nanoparticles coated with mesogenic thiols and studied the behavior of doped nematic, smectic, and cholesteric phases,[67] from compounds such as **23**. In particular, the stabilizing mesogenic cyanobi-

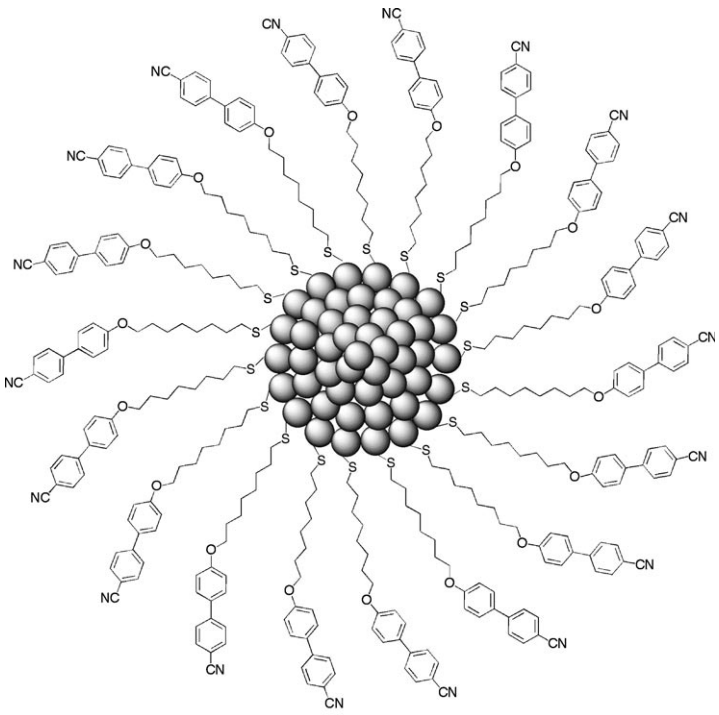

23

phenyl-terminated thiols chosen were designed to match perfectly the chemical nature of the liquid-crystal solvent to be used to increase solubility and avoid the possibility of separation as a result of chemical incompatibility of the particle and solvent.

These nanoparticles are highly soluble in the liquid-crystal solvents studied without the need of sonication, giving dark brown solutions. They show complex thermal behavior near to the nematic to isotropic liquid transition, which is reminiscent of the phase behavior of the nematic phase of silicone oil colloidal dispersions in E7 reported by Poulin et al.,[48] but in the present case the particles are a similar size to the liquid-crystal solvent molecules. Moreover, this behavior matches very closely the theoretically predicted phase diagram of a mixture of hard particles in a nematic phase at high weight fraction of mesogen.[68]

Thus through the processes of self-assembly and self-organization, liquid-crystalline phases have opened up new perspectives in materials science towards the design and engineering of supramolecular materials.[69] The self-organization in two- and three-dimensional space offered by the liquid-crystalline medium is an ideal vehicle to explore and control the organization of matter on the nanometer to the micrometer scale, which is the key to the development of nanotechnology.

3. Liquid-Crystalline Super- and Suprastructures

Probably the best examples, and possibly the most numerous, of material systems that self-assemble and then self-organize to form liquid crystals are those based on hydrogen-bonding. Classical examples include the 4-alkoxybenzoic acids, the 2-alkoxynaphthoic acids,[70] and diisobutylsilanediol (**24**).[71]

Diisobutylsilanediol, **24**, epitomizes the self-assembly–self-organization approach to the formation of a liquid-crystalline phase. As a molecular entity, **24** would be a very unlikely candidate to form any type of liquid-crystal phase. It is globular in shape, with little flexibility. However, when it dimerizes it forms a disclike self-assembled structure $(\mathbf{24})_2$,

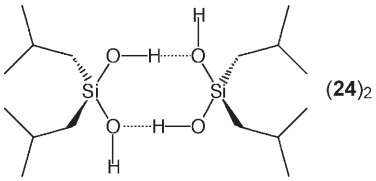

$(\mathbf{24})_2$

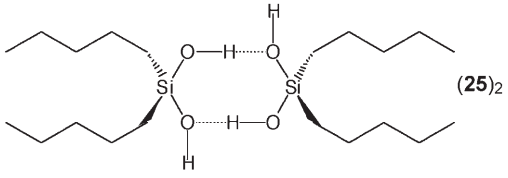

$(\mathbf{25})_2$

which can in turn hydrogen-bond with other dimers to form a supramolecular columnar structure and thereby create a superphase as described by Zocher et al.[18] Furthermore, **24** demonstrates the importance of the interactions stabilizing a so-called superphase. Firstly, if other substituted silanediols are investigated it becomes apparent that the isobutyl chains are critically important to mesophase formation as no other homologues or isomers of **24** form mesophases. For example dibutylsilanediol (**25**) is non-mesogenic.[72] Consequently, the

shape of the diisobutyl unit is an essential aspect of the self-assembly–self-organization process. The diisobutyl chains effectively fill the space around the hydrogen-bonded network, uniquely spacing the disclike dimers one on top of another allowing the columnar structure to be stabilized. Thus diisobutylsilane diol has the ideal shape to allow the formation of dimers to occur, which in turn have a suitable topology for the favorable interactions that allow for the stabilization of columnar mesophases. Thus, shape, topology, polarizability, hydrogen-bonding, and van der Waals interactions combine in the formation of the mesophase.

For dibutylsilanediol (**25**) the dimer is not able to form a space-filling aliphatic sheath around the hydrogen-bonded siloxane network, and so a columnar structure would not be stabilized and mesophase formation does not occur. Other aliphatic substituents, for example, cyclohexane, are too bulky, thereby suppressing dimer formation, and again creation of a mesophase is not possible.

Although the organization of the individual molecules in the liquid-crystal phase of diisobutylsilanediol (**24**) is portrayed as being static, this is not the case in reality. The hydrogen-bonding is mobile, and the dimers fluctuate as a result of the individual atoms and functional groups rotating and oscillating. In addition, the columns will move past one another in the columnar phase. Thus, diisobutylsilanediol is a unique example of a supramolecular self-assembling–self-organizing system that forms a supermesophase.

3.1. Self-Assembly and Self-Organization in Glycolipids

In recent years there have been many reports on lipid systems, most notably glycolipids, which are capable of hydrogen-bonding and which exhibit supermesomorphic thermotropic phase behavior.[73] Most simple glycolipids exhibit layered smectic phases where, as with diisobutylsilanediol, the individual molecular glycolipids would be very unlikely candidates to form any type of liquid-crystal phase without the process of self-assembly accompanying self-organization. Figure 17 shows the process of self-assembly and mesophase formation for a simple glycolipid. In this case the individual molecules form a dynamically fluctuating hydrogen-bonded network. The mesophase structure can thus be considered as a microphase segregated between the weakly interacting aliphatic chains and the more strongly hydrogen-bonded network.

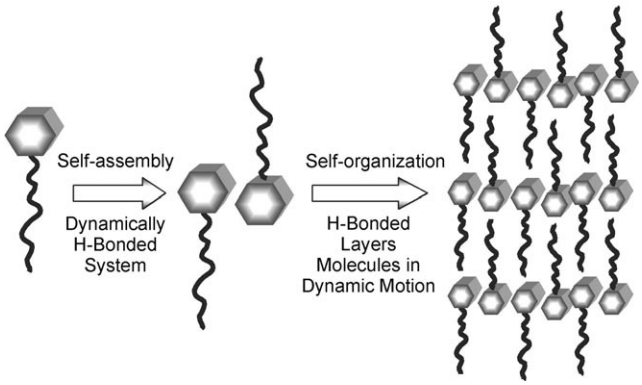

Figure 17. A typical structure for the thermotropic smectic A phase of a glycolipid.

3.2. Curvature and Molecular Packing in Glycolipids

In typical non-amphiphilic thermotropic liquid-crystal systems, it is common to develop property/structure correlations through the investigation of the variation in transition temperature(s) as a function of systematic changes in molecular structure.[74] Usually, it is found that the clearing-point and liquid-crystal-to-liquid-crystal transition temperatures are extremely sensitive to small structural changes at the molecular level, and, in fact, many studies have been made in relation to the effects of substituent size and position on mesomorphic properties. However, similar studies for glycolipids with respect to their thermotropic behavior are relatively few. One such comparison has been completed for the thermotropic properties of the *O*-dodecyl α,β-D-glucopyranoses by several research groups including that of Miethchen.[75] Miethchen et al. demonstrated the effect on clearing-point temperatures as a dodecyl chain was moved sequentially from one position to the next in substituted D-glucopyranose systems (Scheme 3). The ratio of α to β anomer for this series of materials varies from one member to the next, except for the 1-*O*-substituted isomer in which either 100% α or 100% β anomer is present. Despite a superimposed effect of the variation of the anomeric purity across the series, the wide range in clearing points from 140 to 167.2 °C clearly is predominantly influenced by the position of substitution.

Interestingly, the mesophase exhibited by all of the isomers is the same; a smectic A_d* phase in which the molecules have an interdigitated arrangement within the layers where the ratio of layer thickness to molecular length is 1.4:1. The fact that the mesophase type is lamellar suggests that for each of the members of the series molecules are rodlike in shape, with the carbohydrate head group having a similar cross-sectional area to the aliphatic chain. However, when the cross-sectional area of the head group (carbohydrate residue) is larger than that of the aliphatic chain, or vice-versa, then there is the possibility that packing of the molecules induces a natural curvature (Figure 18). The curvature in the packing of the molecules can induce the formation of columnar and cubic phases.[76]

To extend the relationship between the cross-sectional area of the head group and that of the aliphatic chain the effect on mesomorphic properties of the position of substitution of an aliphatic chain was examined in disaccharide systems. By introducing a disaccharide unit it was predicted that the relative cross-sectional area of the sugar head group would vary considerably as the aliphatic chain was "moved" sequentially from one position to the next.

Although the family of mesogenic glycolipids, which have molecular architectures composed of a pyranose, furanose, or acyclic monosaccharide unit and a single alkyl chain, is growing, the number of mesogenic glycolipids that have head

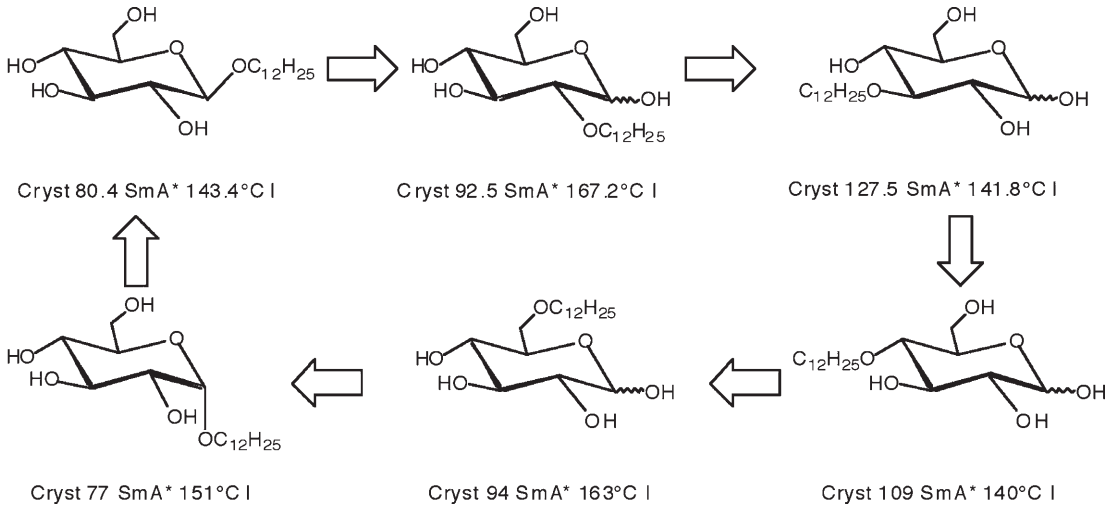

Scheme 3. Effect of position of substitution of a dodecyl aliphatic chain on the liquid crystal properties of *O*-dodecyl-α,β-D-glucopyranoses.

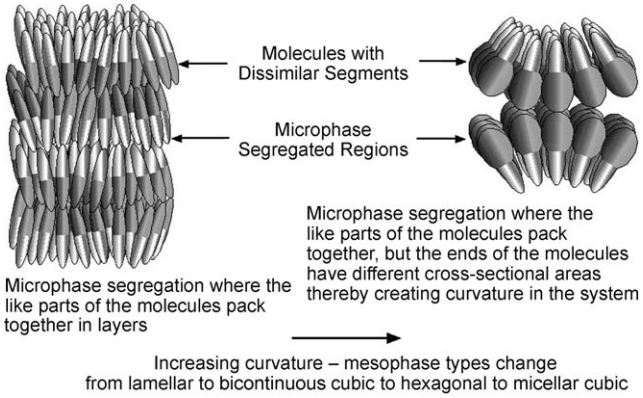

Figure 18. Effect of curvature of packing on mesophase formation.

groups that have two or more sugar units bonded to each other in a linear or branched fashion remains relatively small. For example, most of the mesogenic disaccharide compounds synthesized have been derived from reducing disaccharides, such as maltose and lactose.[77] Dodecyl β-D-maltoside (**26**) and tetradecyl β-D-lactoside (**27**) were each found to exhibit a bilayer smectic A^*_d phase.[78] Dodecyl-α-gentiobioside (**28**) on the other hand, was found to exhibit a cubic phase.[79] The position of both the alkyl chain and the linkage between the two sugar units engenders a nonlinear molecular structure. Therefore, in this case, the material self-organizes to give a cubic phase, where curvature of the local molecular packing is present.

In a similar way, a dodecyl chain was sequentially moved from one position to the next in the mono-*O*-(2-hydroxydodecyl)sucrose family of materials and the liquid-crystal behavior of the materials was examined.[76] Sucrose itself provides a unique opportunity to study the combination of a pyranose and a furanose ring system. Comparisons have already been made on furanose- and pyranose-based glycolipids which have a single sugar unit in the head group, these have shown that the clearing points of the α and β anomers have an inverted relationship with respect to the ring type of the sugar moiety.[80]

Figure 19 shows the structure of the family of sucrose ethers examined. The 2-hydroxydodecyl chain was sequentially moved from position **a** to **g** and the liquid-crystal properties of the materials were examined by microscopy, differential scanning calorimetry (DSC), and miscibility studies. Molecular modeling was used to examine the molecular shapes of the isomers. Where the aliphatic chain is attached to positions **b**–**e**, or **g** the shape of each associated molecular structure is rodlike, however, for positions **a** and **f** the molecular structures become T-shaped with the cross-sectional area of the head group being larger than that of the aliphatic chain. Consequently, with **a** and **f** having T-shaped (wedge-shaped) structures they exhibit cubic and columnar phases, respectively. The changeover from one type of phase to another, that is, lamellar to columnar, also involves a large change in clearing-point temperatures. The columnar and cubic phases tend to occur at much lower temperatures, approximately 50 K lower than the lamellar phase (Figure 20).

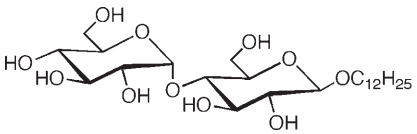

Cryst 80 SmA^*_d 244 °C I

26

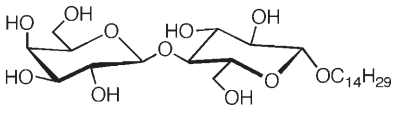

Cryst 183 SmA^*_d 246 °C I

27

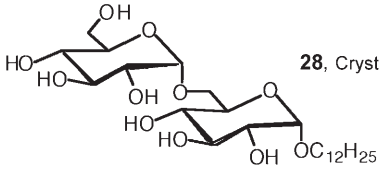

28, Cryst 75 Cub 162 °C I

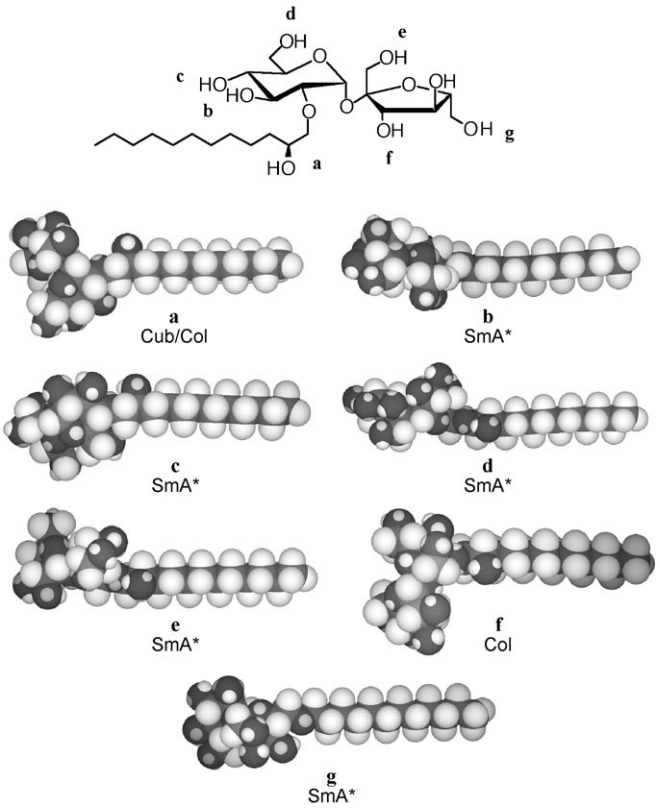

Figure 19. Effect of the position of substituents on the molecular shape of the mono-*O*-(2-hydroxydodecyl)sucroses (dark gray O, mid-gray C, white H).

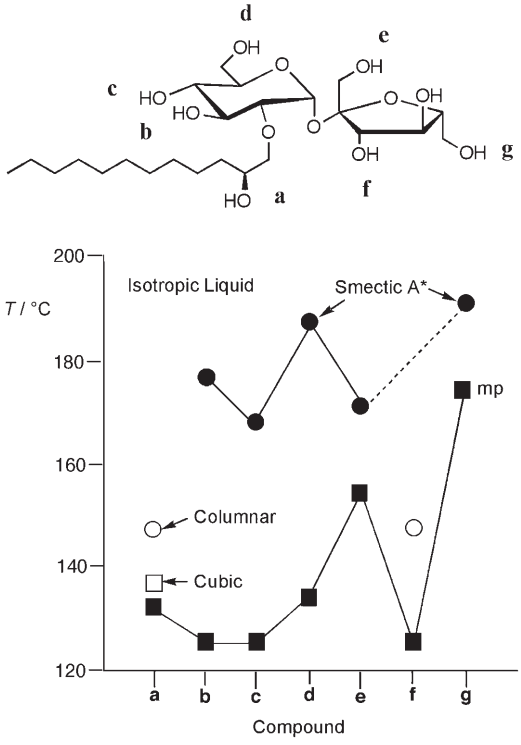

Figure 20. The relative transitions for the mono-*O*-(2-hydroxydodecyl)-sucroses: ■ melting points, □ col to cubic, ○ col to isotropic liquid, ● SmA* to isotropic liquid.

The balance between the formation of lamellar, columnar, or cubic structures is finely tuned. For example, the difference between axial and equatorial substitution, or even whether or not a hydroxy group is axial or equatorial can be enough to tip the balance in favor of one phase or another. Dumoulin et al.[81] showed by optical microscopy, differential scanning calorimetry, and X-ray diffraction that 4-[4-(didodecylamino)phenylazo]phenyl-β-D-glucopyranoside exhibited a columnar phase, whereas 4-[4-(didodecylamino)phenylazo]-phenyl-β-D-galactopyranoside gave a lamellar phase. It was envisaged that for the glucose derivative, curvature is induced within layers, becoming localized into a columnar structure, whereas for the galactoside any curvature is not strong enough to stabilize columnar ordering, as shown in Figure 21.

3.3 Intramolecular Hydrogen-Bonding and Superstructures in Glycolipids

Another possibility of stabilizing columnar or cubic phases over lamellar phases is to change the length of the aliphatic chain(s). For a material which has a head group that has a larger cross-sectional area relative to the aliphatic chain, then, as the chain is increased in length lamellar phases will become more stable because the effect of curvature in the packing of the molecules will be reduced, that is, the molecules become less wedge-shaped. However, for systems that have a larger cross-sectional area for the hydrophobic region relative to the head group, the longer the aliphatic chain(s) the more stable the columnar and cubic phases become. Molinier et al.[76b] demonstrated the effect of aliphatic chain length by comparing the liquid-crystal properties of 6-*O*-octanoylsucrose (**29**) with 6-*O*-octadecanoylsucrose (**30**; Figure 22). Molecular simulations (at absolute zero in the gas phase) show that the sucrose head groups form intramolecular hydrogen bonds, thereby exposing the remaining hydroxy groups on the outer surface of the head. The models show that for the shorter chain length, the overall molecular structure is wedge-shaped, whereas for with a longer chain the overall structure is more rodlike. Figure 22 indicates that the clearing point for the lamellar phase is over 100 K higher than that for the columnar phase, which is in keeping with the results obtained for the mono-*O*-(2-hydroxydodecyl)sucrose family of materials described in Section 3.2.

Intramolecular hydrogen-bonding can thus affect the molecular shape and topology, thereby influencing the self-assembly and self-organization properties. Molinier et al.[76b] went on to investigate the liquid-crystal properties of three families of materials, the 6-, 6′-, and 1′-*O*-alkanoylsucroses. For all three families, simulations show that intramolecular hydrogen-bonding is a low-energy conformation which leads to the formation of quasi-macrocyclic structures (Figure 23). By forming cyclic structures, the sucrose head groups have the maximum number of hydroxy groups on the surface furthest away from the aliphatic chains. In this way the head groups can be easily solvated with water to form lyotropic systems.

The formation of macrocycles for the three families also leads to the possibility of creating cavities within the molecular structures (see Figure 23). The macrocycles have

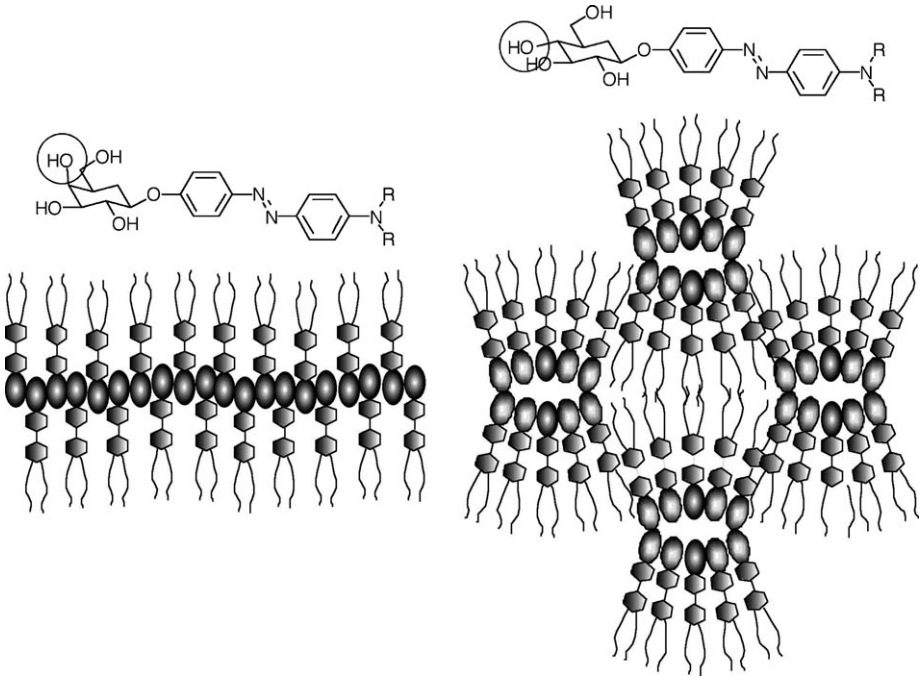

Figure 21. Formation of a columnar mesophase for 4-[4-(didodecylamino)phenylazo]phenyl-β-D-glucopyranoside (right) and formation of a lamellar mesophase for the corresponding β-D-galactopyranoside (left). R: $C_{12}H_{25}$.

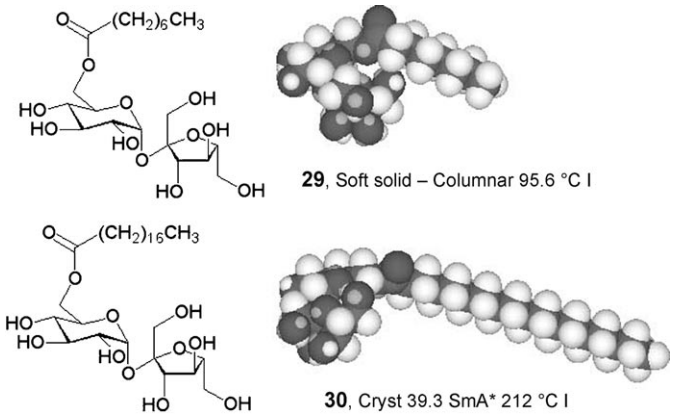

Figure 22. Comparison of the molecular shapes of 6-*O*-octanoyl- (**29**) and 6-*O*-octadecanoylsucrose (**30**; dark gray O, mid-gray C, white H).

either five or six oxygen atoms in their ring structures which would allow for complexation of various ions. When these systems form columnar phases, with the head groups located at the surfaces of the columns and the aliphatic chains directed towards the interior, the macrocyclic rings/cavities will overlap, or stack, one on top of another, thereby forming tubes, or ion channels, through the structure (Figure 24).

3.4. Complex Lamellar Structures in Sucrose Systems

Molinier et al.[76b] developed their research into the self-organizing properties of sucrose-based lipids through the preparation and characterization of the 1′,6′ and the 6,6′ disubstituted sucrose esters **31** and **32**. Some examples of these two families of materials had been reported previously, but their liquid-crystal properties were not investigated. Bottle and Jenkins[82] had already shown that 6,6′-di-*O*-palmitoylsucrose (**33**) exhibits biological activity and has immunostimulant properties. The structure of **33** is similar to that of Cord Factor (6,6′-dimycolic ester of α,α-trehalose (**34**)). Cord Factor has been shown to have immunostimulant properties and antitumor activity, and is responsible for bacteria forming cords in aqueous media. Cord Factor is also associated with virulent strains of *tubercle bacilli*.[83]

We focus first on liquid-crystalline behavior of 6,6′-di-*O*-octadecanoylsucrose (**35**) A material with quite remarkable structural properties. The material exhibits a smectic A* phase as predicted, however, the variation of the layer spacing d as a function of temperature is unexpectedly large. The layer spacing is shown in Figure 25 as a radially integrated diffraction pattern taken over a temperature range of 40–200 °C. An intense small-angle reflection was observed in the isotropic phase (the first light-gray curves in Figure 25), which indicates pre-transitional effects occurring in the liquid, and might be related to clusters of molecules in which intermolecular hydrogen bonding is present.

When cooling down into the smectic A* phase (dark lines in Figure 25) the second-order reflection (002) can be seen, which grows more intense as the temperature falls. At higher temperatures the fundamental (001) reflection was fitted by a Lorentzian distribution function, taken from the widths of the peak-intensity values at half the peak height, indicating short-range positional order. At lower temperatures ($T < 100$ °C), the shape of the reflection changes to a Gaussian distribution function, indicating an increase in the extent of the positional order. In this temperature range, third- and fourth-order reflections were also observed, indicating that the layers become better defined. The change in shape of the diffraction patterns for the fundamental reflections at $T = 105$ °C (Lorentzian) and $T = 95$ °C (Gaussian) is illustrated in Figure 26a.

A strong temperature dependence of the layer spacing was also observed in the smectic phase, with the d-values ranging from 35 to 50 Å (Figure 26b). Remarkably, the d-spacing changes continuously in the smectic phase and into the isotropic liquid. Crystallization is observed between 70 and 75 °C, where the layer spacing (d_{001}) and the correlation length (the half-width of the reflection; ξ_{001}) become virtually temperature independent. Where the peak shape changes from Gaussian to Lorentzian ($T = 100$ °C) on heating, a local minimum in the correlation length was observed, which marks a change in the form/structure of the smectic A* phase.

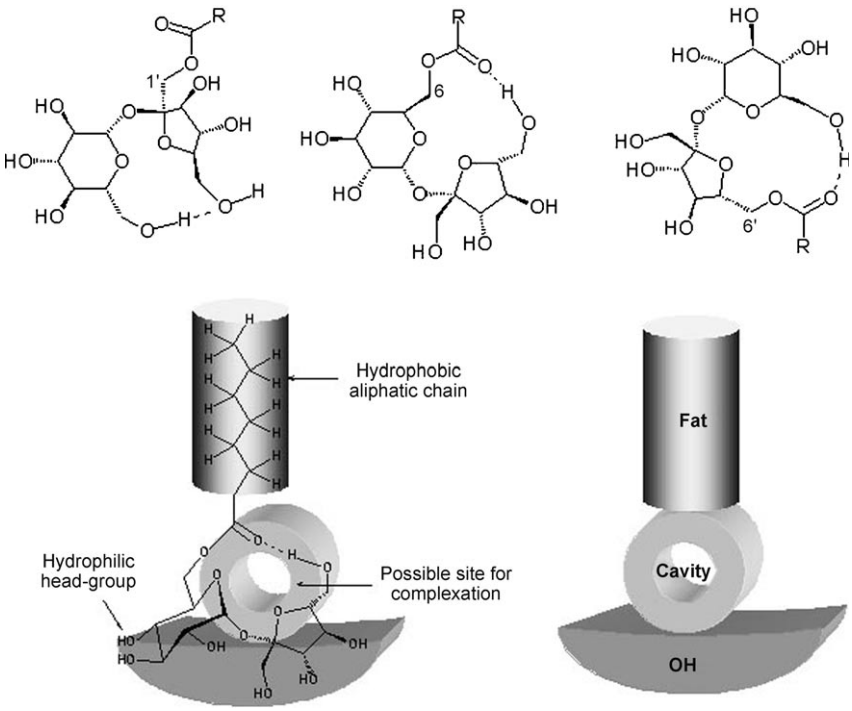

Figure 23. Intramolecular hydrogen bonding in *O*-alkanoylsucroses results in cyclic systems in which the hydroxy groups are exposed on the outer surface of the head-groups.

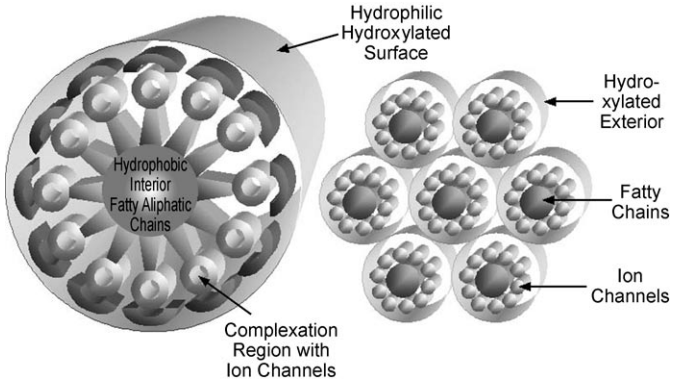

Figure 24. Columnar stacking of the intramolecular-hydrogen-bonding-stabilized macrocyclic sugar systems. When the columns pack together they form a hexagonal columnar phase.

At low temperatures the layer spacing approaches 48 Å. Molecular modeling using ChemDraw 3D Ultra gives a length of the minimized extended molecular conformation of 54.8 Å, and Dreiding Molecular Models give a value of 56 Å. At high temperatures the layer spacing approaches 36 Å, whereas modeling of the folded molecular conformation gives a value of 31.6 Å, and Dreiding Models a value of 29.7 Å. Figure 27 shows together the fully extended and folded structures.

One explanation given for the transition in the smectic A* phase was that the molecules are interdigitated, and the extent of the interdigitation reduces with temperature as the phase becomes more ordered. Thus, it appeared from the d-spacing measurements that there was a continuous transformation from an intercalated SmA^*_c[84] to a non-intercalated SmA^*_1 structuring of the layers. The transformation from the intercalated to the non-intercalated was thought to be related to the change in Lorentzian to Gaussian line-shape associated with the correlation length.

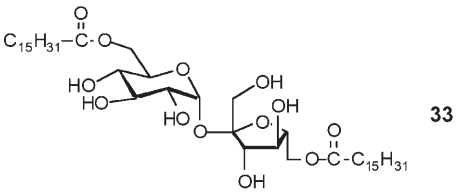

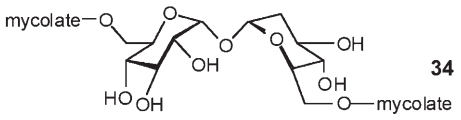

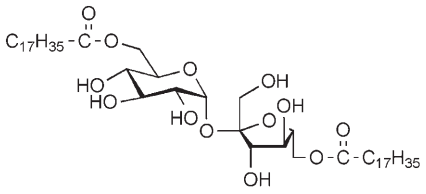

35, Cryst 109.8 SmA* 164.3 °C I Recryst 70 °C

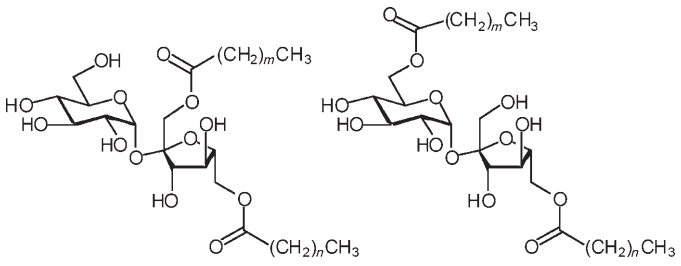

1',6'-diesters **31** 6',6'-diesters **32**

An alternative explanation was that the molecules have folded conformations, and at high temperatures the folded molecules pack in interdigitated bilayers, that is, as in the SmA^*_d phase.[85] As the temperature is lowered the interdigitation is reduced and eventually the phase has only weak interdigitation, as in the SmA^*_2 phase. The change over from one form of smectic A* phase to the other may not be detected from the X-ray layer spacings, but it is possible that

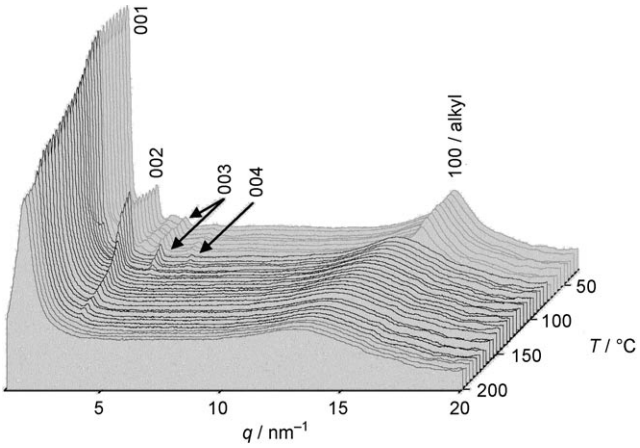

Figure 25. Radially integrated diffraction pattern of **35** taken over a temperature range of 40–200 °C. The diffraction intensities are given in a logarithmic scale.

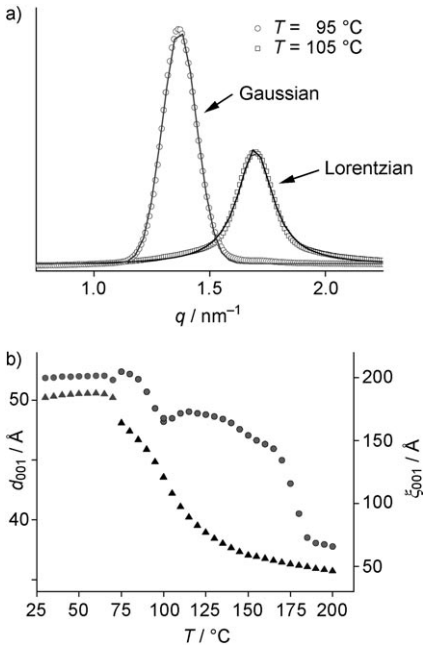

Figure 26. a) Lorentzian (black) and Gaussian (gray) fits to the diffraction data of **35** at temperatures of 105 (□) and 95 °C (○). b) Temperature-dependence of the layer spacing, d_{001} (▲), and the correlation length, ξ_{001} (●) of **35**.

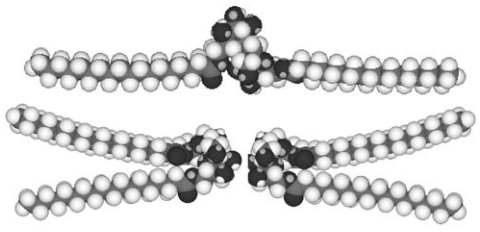

Figure 27. The fully extended structure (top, one molecule), and the folded structure (bottom, two molecules) for **35**; dark gray O, mid-gray C, white H.

such a transition might be seen through examination of the correlation length. The change in the correlation length is also associated with an increase in the number of reflections seen in the radial scans. At high temperatures only the first- and second-order reflections are seen, whereas at low temperatures the number of reflections increases to the fourth-order reflection. This situation suggests that the layers in the smectic A* phase are becoming better defined at lower temperatures. The increased layer definition may be a result of the sugar units packing more strongly together as a result of extensive hydrogen-bonding interactions.

The second model described above is more likely to give well-defined layers than the first model, because the second arrangement allows for flexible interactions both between and within the layers, whereas the interlayer ordering for the first model has a greater dependency on the interfacial interactions between the aliphatic chains. Nevertheless, whichever model is applied, such a substantial change in the layer spacing in a smectic A* phase as a function of temperature has not been observed before in conventional thermotropic liquid crystals, and smectic A* polymorphism has not been observed before in sugar-based mesogens.

A comparison of the layer spacings as a function of temperature for the octanoyl, hexadecanoyl, and octadecanoyl homologues of **32** (Figure 28) clearly demonstrates, for

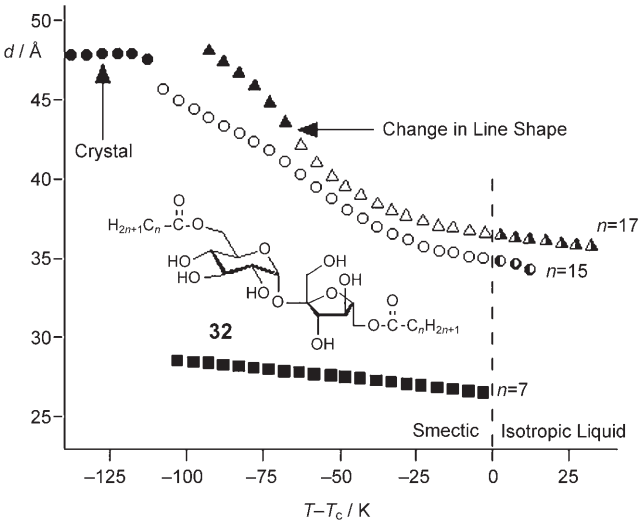

Figure 28. The layer spacing as a function of the reduced temperature from the clearing point ($T-T_c$) °C for the octanoyl, hexadecanoyl, and octadecanoyl homologues of **32**.

the materials with shorter aliphatic chains, that the layer spacing is relatively independent of temperature, whereas the longer chain lengths show very large temperature dependencies. Moreover, the temperature dependency increases with increasing aliphatic chain length. In addition, for the longer chains the layer ordering persists well into the liquid phase. Thus, it is the self-assembly that creates supramolecular structures with topological forms suitable to support mesophase stability. The self-assembly may just be dimerization it may occur through the clustering together of many subunits,

or indeed it may be as simple a process as intramolecular hydrogen-bonding.

4. Transmission of Structural Information

The basic molecular design of liquid crystals with rodlike molecular structures usually involves the incorporation of a central aromatic or heterocyclic core unit which is sandwiched between two terminal aliphatic chains.[74] When molecules with this type of architecture self-organize they do so with their rigid, aromatic parts tending to pack together and the flexible/dynamic aliphatic chains orienting together. Thereby the overall system becomes locally microphase segregated. This design technique has, thus, been used very successfully in the development of liquid crystals for display applications, for example, the twisted nematic displays (TNLCDs) found in watches, clocks, mobile telephones, and computer displays, the vertically aligned nematic displays (VANLCDs) found in modern television screens, and the surface-stabilized ferroelectric displays (SSFLCDs) found in the eyepieces of digital cameras.

4.1. Synclinic and Anticlinic Mesomorphic Superstructures

The main target of liquid-crystal material design has been, by default, the variation in the structure of the central core region of the molecules, in the belief that the core is more important in influencing mesophase incidence, mesophase temperature range, isotropization point, melting point, mesophase sequence, and the reorientational viscosity associated with the mesophase. Only a few studies have been reported where the terminal positions of the aliphatic chains have been manipulated. Through these limited, and unsystematic, studies there has been a realization, that small changes to the termini of the molecular structure have a marked effect on liquid-crystal phase formation and related physical properties.

For example, consider the structure of the smectic C phase, in the synclinic variant the constituent molecules are arranged in diffuse layers in which the molecules are tilted at a temperature-dependent angle with respect to the layer planes. The molecules within the layers are locally hexagonally close-packed; however, this ordering is only short range, extending over distances of approximately 15 Å. Over large distances the molecules are randomly packed, and in any one domain the molecules are tilted roughly in the same direction, both in and between the layers (see Figure 29). Thus, the tilt orientational ordering between successive layers is preserved over long distances.

The anticlinic variant of the smectic C phase has an in-plane ordering of the molecules which is thought to be identical to that of the synclinic smectic C phase. The major difference between the anticlinic C phase and the synclinic smectic C phases resides in the relationship between the tilt directions in successive layers. In the anticlinic phase the tilt direction is rotated in the opposite direction on passing from one layer to the next. The tilt direction appears to flip from one layer to the next, and thus the optic axis of the phase is

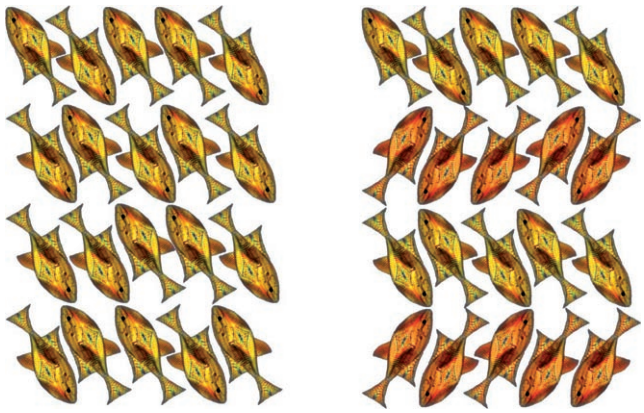

Figure 29. Structures of the synclinic (left) and anticlinic smectic C phases (right). The molecules are typically represented with fish-like shapes. When the "fish" are chiral, the phases become ferroelectric and antiferroelectric, respectively.

effectively normal to the layer planes (Figure 29). To date, for compounds that exhibit both phases, the anticlinic smectic C phase has always been found to occur at a lower temperature than the synclinic smectic C phase.

When a material forming a synclinic phase is chiral then the mesophase becomes ferroelectric (P_s is finite), and when it forms an anticlinic structure the phase becomes antiferroelectric ($P_s = 0$). Controlling the molecular tilt directions between layers thus becomes particularly important for the development of fast-switching light valves, photonic switches, and displays. It has been found that the local director can be controlled from layer to layer through judicious design of the end groups. Most notably, the orientation of the terminal group, that is, its presentation to adjacent layers, and its ability to interact with the neighboring layer are the important factors in determining the tilt orientation on passing from one layer to the next in a bulk sample.[86,87]

For example, consider the terphenyl derivatives shown in Scheme 4. All of the materials have the same structure except for the right-hand terminal chain. All members of type **36** have an ether linkage joining the terminal chain to the terphenyl core. For type **37**, the linking unit is an ester. The angle that the terminal group is attached to the core also affects the angle by which the terminal group interacts with the adjacent layers. Bartolino et al.[12] showed that these molecules, which generally have zigzag shapes, are oriented within the layers so that the cores are more tilted than the tails. Regardless of whether the materials are non-chiral (type **36a** and type **37a**), racemic, or chiral (type **36b** or type **37b**) the terminal chains clearly have different orientations relative to the layer interfaces, with the ether groups being predominantly synclinic, whereas the ester groups are anticlinic.

The relationship between terminal ethers and esters in their abilities to form synclinic versus anticlinic phases has been known for many years, however, this work was mostly confined to the study of the properties of biphenylyloxy benzoates (see Scheme 5), which are not stable for practical devices, such as projection displays. Difluoroterphenyl compounds, on the other hand, are very stable materials with suitably desirable physical properties for use in ferroelectric

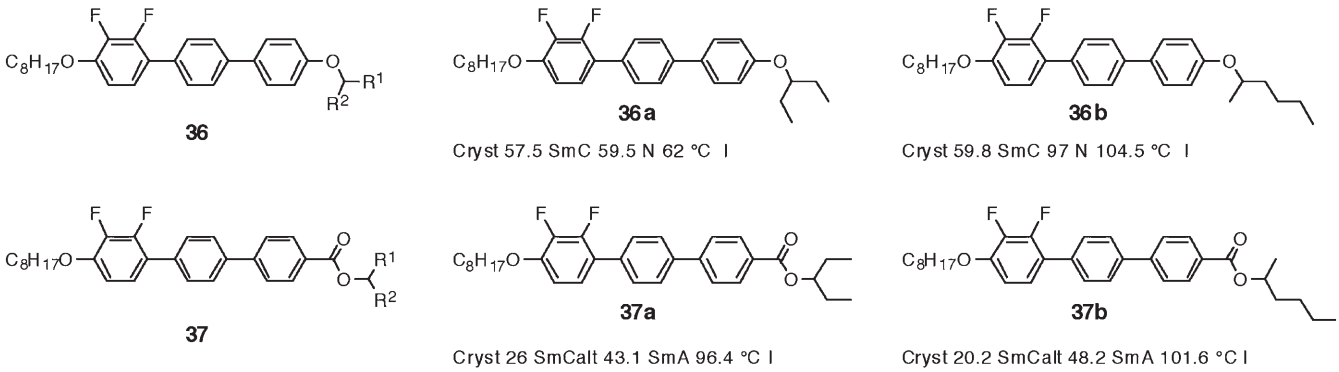

Scheme 4. Comparison of transition temperatures and mesophase sequences of terphenyl ethers **36** versus terphenyl esters **37**.

applications. However, without the use of terminal controlling groups it is very difficult to induce the formation of anticlinic phases in these materials. Through the judicious choice of various terminal groups it has become apparent that a wide variety of mesophase types and sequences could be controlled by this methodology, and indeed under certain circumstances novel phases could be observed.

Figure 30 shows a comparison between how a normal smectic layer might appear, in this case smectic A, (Figure 30a), and how the interlayer organization might appear with the incorporation of "structure-control" groups, shown as black discs, at the terminal positions. Figure 30b shows the structure of the mesophase with as many molecules pointing "up" as there are pointing "down" and homogeneously distributed within the layer. Structural variations could exist, at one extreme clusters of "up" and "down" molecular species form an inhomogeneously ordered system (rafts or swarms; Figure 30c), at the other, fully 2D modulated structures occur (Figure 30d). All of these arrangements would, of course, have profound effects on mesophase structure, the arrangements of the molecules in their layers, and the ensuing physical properties.

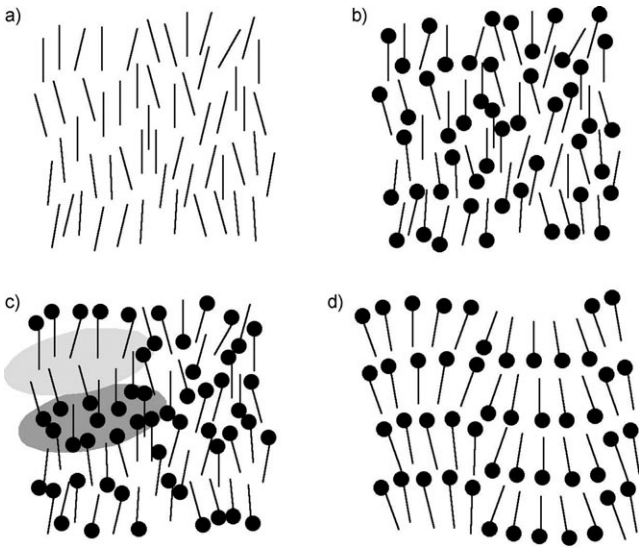

Figure 30. a) The disorganized layer structure of a typical smectic A phase with the molecules shown as rods; b) the disorganized layered structure of a smectic A phase in which the molecules have bulky end groups; c) clustering of tails and head groups (rafts) to give an inhomogeneous layer structure (highlighted in gray); and d) in-plane ordering of the molecules caused by the curvature induced through the packing together of the bulky end groups, the modulation could be one-dimensional or two dimensional within the layer.

Taking this approach, two other issues are of interest, 1) where the terminal groups are chiral, the interfaces between the layers become chiral, and so behave like chiral molecular recognition surfaces,[87] and 2) where clusters form within the layers templating can occur from one layer to the next leading to "raft-like" structures in layered phases.

Where there are chiral recognition surfaces, intermediary phases, such as the ferrielectric phases 1 and 2, can occur. For many years there has been a debate over whether or not ferrielectric phases are based on Ising structures[88] (see Figure 31, top), or short-pitch helical twist structures that give 360° of twist over three to four layers, the so-called "Clock model"[89] (see Figure 31, bottom).

In the Ising model, through the periodic incorporation of extra layers, ferrielectric phases can be inserted between the ferroelectric and antiferroelectric phases in the temperature/structure phase diagram. Thus tilting to the "left" or tilting to the "right" can be found in incremental steps, for example, 2:1, 3:1, 4:1. In this way a number of ferriphases were proposed to occur in which the spontaneous polarization, P_s, had a specific non-zero value. Where the left–right steps are incommensurate, a "Devil's staircase" structure of uneven steps is formed.

The "Clock model" on the other hand involves a rotation of the tilt on passing from one layer to the next. The rotation angle was found by resonance X-ray scattering to be approximately 90° for one ferriphase and 120° for another ferriphase. Thus, according to this model, two ferriphases should occur (Figure 31, bottom).

The transmission of structural information across the layers is better supported by the Clock model than the Ising model for the following reasons; 1) the ferrielectric phase requires the liquid-crystal material to be chiral, and thus the layer surface interfaces will exhibit chiral recognition and templating. The Ising model because of the 180° rotation of the tilt does not require a chiral recognition surface, and 2) for the same reason, the Ising model should produce a mesophase

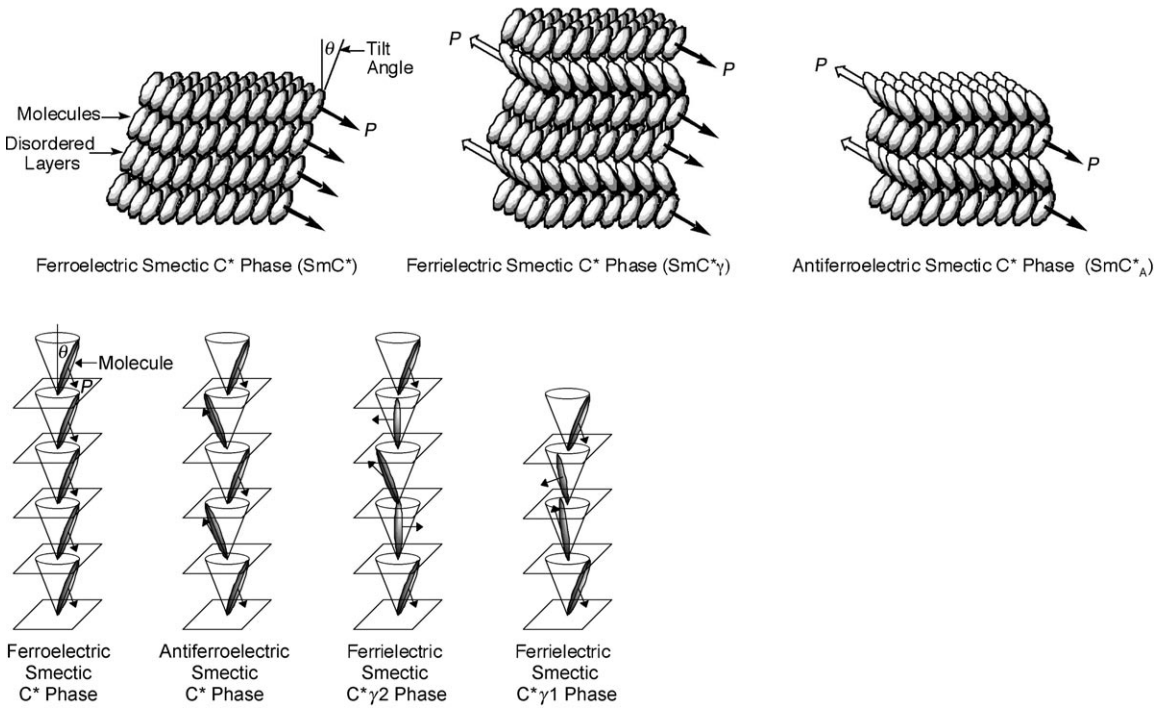

Figure 31. Top: The structures of the ferroelectric (maximum polarization *P*), ferrielectric (intermediate polarization), and antiferroelectric (zero polarization) phases. The ferrielectric phase shown has an Ising 2:1 structure. Bottom: the Clock models for the ferro-, ferri-, and antiferroelectric phases. The molecules are shown as elliptical rods.

that is equivalent to the ferrielectric phase for non-chiral materials, whereas the Clock model cannot support such a mesophase formation as there will be an equal opportunity to twist to the left or right and annihilation of the structure will occur. To date no achiral liquid crystals have been found to exhibit a ferrielectric phase.

Scheme 5 shows how the structure of a biphenylyloxy benzoate based family of materials can be manipulated through changes to the core system and to the terminal end groups to favor synclinic ferroelectric or anticlinic antiferroelectric phases, and to suppress the ferrielectric phases which are disfavored in device applications.[90] The chemical structure of the aromatic core system can be manipulated by the incorporation of polar groups, such as fluoro-substituents (Scheme 5, compare **A**, **B**, and **C**) so that synclinic properties are preferred. When the polar groups are located towards the center of the core structure (**C**), they can be used to suppress both ferri- and antiferroelectric phases, thereby stabilizing ferroelectric properties. Alternatively, by incorporating longitudinal dipole moments, thereby creating quadrupolar systems, antiferroelectric phases are stabilized (Scheme 5, **D** and **E**). However, by simply altering the terminal group, through the inclusion of siloxane units (Scheme , compare **A** with **F** and **G**) all the other smectic phases can be suppressed except for the ferroelectric synclinic phase. Thus manipulation of the terminal end groups becomes a powerful weapon in material design.

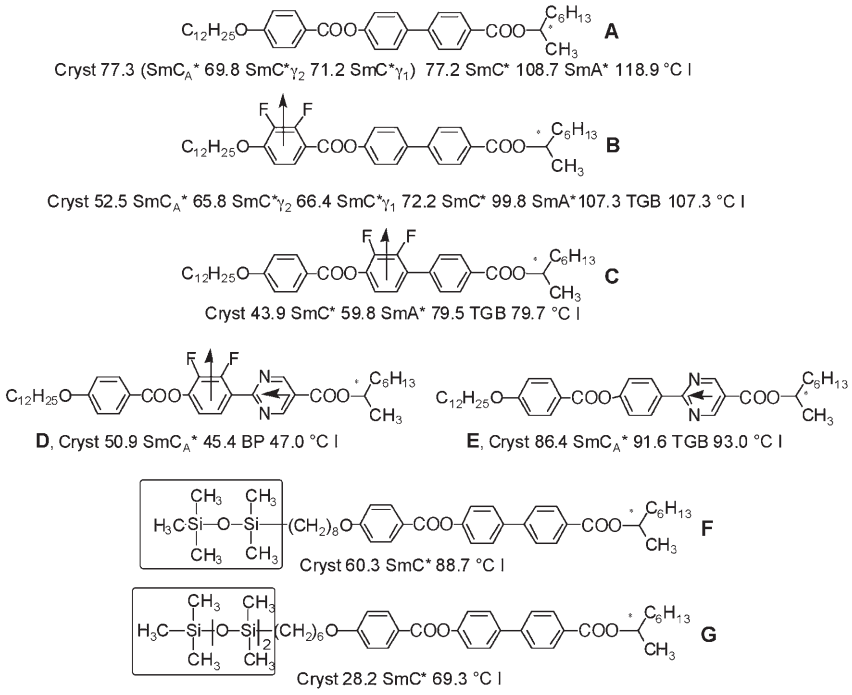

Scheme 5. Effect of changes in molecular structure on the incidence and stability of various smectic phases. The arrows indicate the direction of the molecular dipole. See text for details.

Scheme 6 shows the results of a systematic study of terminal-group structure–property relationships for difluoroterphenyl derivatives. Only one terminal group was varied, terminal position. In comparison to the unsubstituted straight aliphatic chain compounds which exhibit nematic, smectic A, and synclinic smectic C phases, the halogen compounds exhibit only smectic A phases. In other words the substitution with a halogen has the effect of inducing the molecules to "stand up" in the layers rather than tilting over. This effect may be due to strong polar interactions at the layer interfaces caused by the terminal halogen units. Again it appears to be possible to control molecular tilt through changing one atom (halogen for H) at the layer interface.

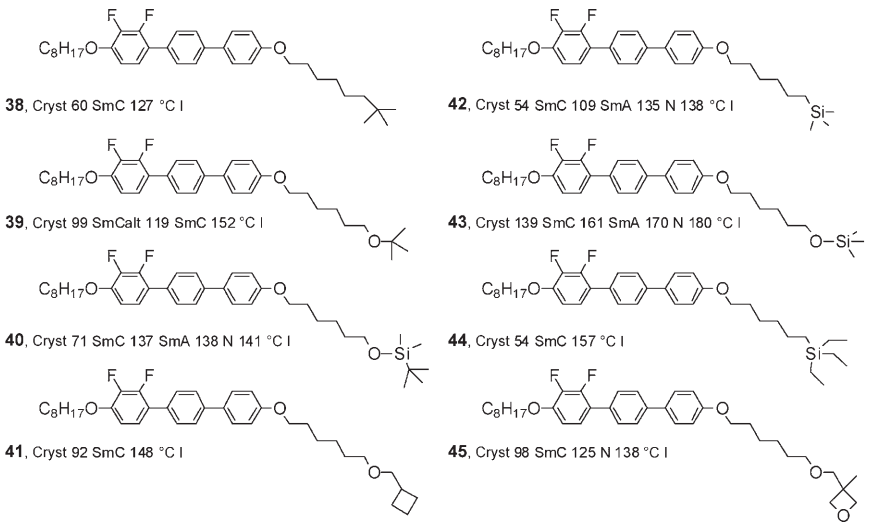

Scheme 6. Structure–property correlation study for difluoroterphenyl derivatives where the terminal end groups are varied.

Understanding the interactions at the interfaces of the layers in lamellar smectic phases is of practical importance in the development of ferroelectric and antiferroelectric optical devices. There are a number of interactions to consider which include the liquid-crystal surface interactions, the penetration of the surface interactions into the bulk of the liquid-crystal phase, the

the rest of the molecular structure was kept the same. All of the materials except for **39** exhibit synlinic smectic C phases. Compound **39** is the only material where an anticlinic phase is formed, and as in the cases described earlier the terminal group points towards the layer interfaces. In particular, and as described previously, terminal silicon-based groups suppress the formation of anticlinic phases, and so compounds **40**, **42**, and **43** exhibit the same phase sequences (N, SmA, SmC). Remarkably these materials exhibit nematic phases which is unusual for compounds with terminal silicon-containing groups. Typically materials with siloxane terminal groups do not exhibit nematic phases and usually have properties more in keeping with compound **44**. If **38** and **42**, and **41** and **45** are compared, it can be seen that the stronger polar end groups induce the formation of nematic phases. Generally, most of the materials that have terminal groups containing exposed heteroatoms, that is, they are not crowded with aliphatic groups, tend to exhibit nematic phases. This property is important when a nematic phase is required to aid in the alignment of a material, for example, for a display device. Thus controlling the structure of the end group can have benefits in practical applications. Conversely, terminal groups that tend to be sterically crowded, such as those found in **38**, **41**, and **44**, do not exhibit nematic phases, they display the same phase behavior, direct isotropic liquid to smectic C phases.

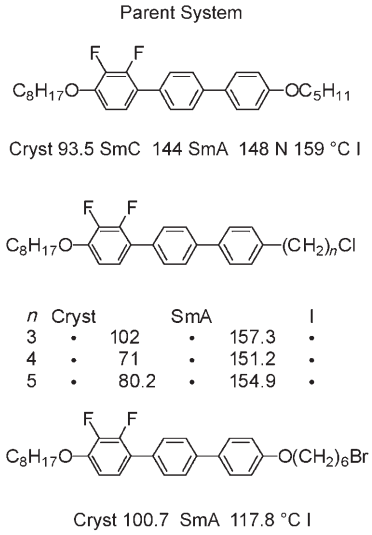

Scheme 7. Effect on liquid-crystalline properties caused by the insertion of a halogen atom at the terminus of the aliphatic chains in substituted difluoroterphenyl derivatives.

4.2. Orthogonal Ordering of the Molecules in Lamellar Phases

Other phases can be stabilized by introducing certain terminal polar groups. Scheme 7 shows a number of compounds where a polar halogen group has been located at the strength of the lateral interactions between the molecules, and the strength of the interactions between the layers (Figure 32). The strength of the surface interactions controls the surface anchoring energies and hence the bistability of the device operation. The strength of the interactions between the layers controls the shape of the hysteresis loop for the ferroelectric phase and of the double hysteresis loop for the antiferroelectric phase. Weak interlayer (out-of-plane) interactions can lead to a collapse of the hysteresis loop(s), and hence markedly affect device configuration, construction, and performance.[90] For example, weak interlayer interactions

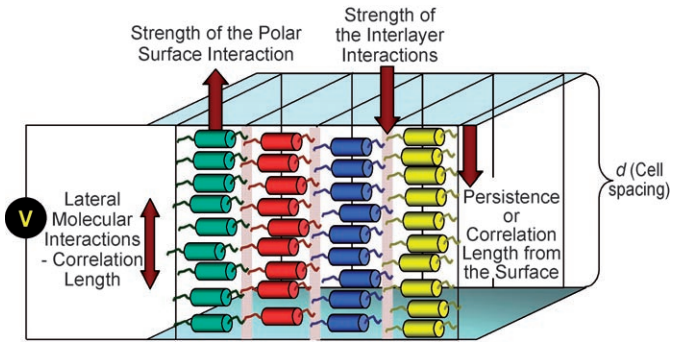

Figure 32. A typical device arrangement for smectic liquid crystals, with the layer planes perpendicular to the cell surface. The important intermolecular and surface interactions are shown.

which lead to the collapse of the hysteresis loop result in a linear electro-optic response to an applied electric field, thereby enabling the device to exhibit a gray-scale response suitable for video-frame rate applications.

Overall, being able to control mesophase structure simply by terminal-group selection is a powerful tool for preparing materials that will induce the selective formation of specific mesophases. This is especially true for lamellar phases, in which the structural information is transmitted across the interfaces of the layers. Indeed, it is the location and shape of the polar and/or bulky terminal groups which define the layer interfaces, and translate the organizational information from layer to layer. Thus the process is one of amplification to the bulk phase.

5. Amplification of Information

The reduced space symmetries associated with liquid crystals can be harnessed to create a range of applications in sensors. The most common sensing application of liquid crystals is provided through the thermochromic effect of the chiral nematic phase.[91] In addition, chiral nematic phases have been utilized as sensory media in investigating the structures and aerodynamics of metal surfaces[92] and as voltage sensors in battery testers.

5.1. Evaluation of Optical Purity using Liquid Crystals

Recently ferroelectric and electroclinic effects have been used to sense chirality and to determine enantiomeric excess of compounds that could be doped in an appropriate liquid-crystal matrix.[93]

It is also well-known that helical macrostructures formed by chiral nematic liquid crystals have the ability to rotate the plane of incident plane-polarized light many orders of magnitude more than equivalent systems in their liquid states. Thereby chiral nematic phases have unique abilities with respect to their amplification of physical properties. Thus, the accurate determination of the change in pitch length of the chiral nematic phase in response to an external stimulus can be used as a sensing method.

Two new techniques have recently been reported that provide a more sensitive measurement of large helical pitch lengths. They employ the measurement of the pitch of a target material by the use of either a twisted nematic cell (TN cell),[94] or a twisted wedge cell.[95]

Accurately constructed TN cells are commercially available from LCD device manufacturers, where they are generally constructed from ITO coated glass with the inner surfaces of the cells coated with polyimide which is buffed. The inner buffed surfaces are arranged so that the buffed directions are perpendicular to one another. Normally, for device operation, a chiral liquid crystal is introduced into the cell to generate a liquid-crystal layer which has a single domain. When an achiral liquid-crystal mixture or a chiral mixture in which the pitch to cell gap ratio is greater than 2 (that is, the pitch is at least double the distance across the cell), is introduced into the cell, the nematic phase will spontaneously form a quarter-helix between the two surfaces (Figure 33). In this arrangement the plane of plane-polarized light is rotated through 90° when it traverses the helical structure.

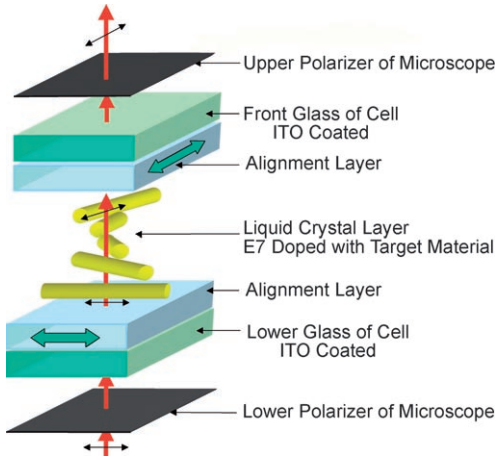

Figure 33. The geometry of a twisted nematic liquid crystal display (TNLCD)—the device is shown with only one twist domain present at zero voltage.

However, the degenerate 90° orientation of the two glass surfaces means that for an achiral material both left- and right-handed quarter helices can be formed. The two domains are separated by disclination defect lines which can be observed by transmitted polarized-light optical microscopy (Figure 34a). The geometrical arrangement of the molecules in the TN device where disclination lines are formed is shown diagrammatically in Figure 34b.

The ability to accurately measure the pitch length of a chiral nematic phase provides an opportunity for the development of a method for determining enantiomeric excess. The method involves doping a target chiral material, which may or may not be a mesogen, into an achiral host nematic liquid crystal, such as commercially available E7 (scheme 8) and measuring the helical pitch length of the resulting mixture. The helical pitch length will be related to the helical twisting power (HTP) and the enantiomeric excess (*ee*) of the

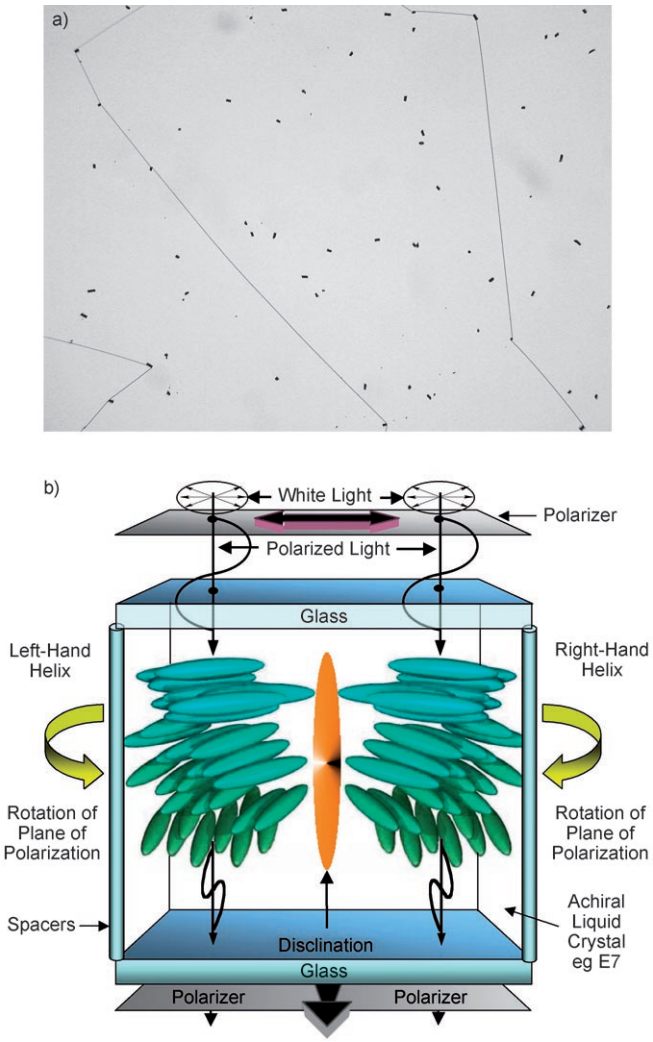

Figure 34. a) Disclination lines separating left- and right-quarter helical domains in E7 achiral host liquid crystal, (magnification: ×100). The black dots are spacers. b) Arrangement of degenerate left- and right-hand quarter helical domains in a TN cell.

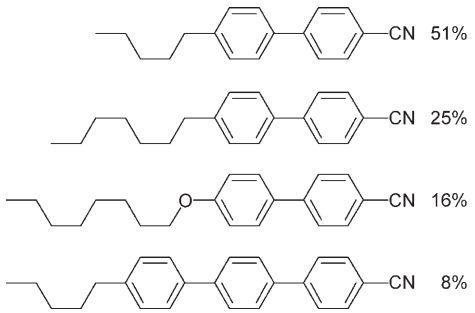

Scheme 8. Composition of the commercial E7 mixture from Merck (wt%).

dopant. Thus for any material, concentration versus reciprocal-pitch-length measurements can be made, and if the HTP is known, the enantiomeric excess can be determined to an accuracy of 0.1%.

Generally, the reciprocal of the pitch as a function of concentration of the dopant is linear for fairly long pitch lengths or low concentration of the dopant. Thus, the presence of a small degree of chirality (e.g. low *ee* value, long pitch, low concentration) breaks the degeneracy in the TN cell one twist area can become favored and grows at the expense of the other. Thus, if the pitch of the nematic phase of the material is less than approximately 0.5 mm only one domain is obtained, whereas for pitches greater than approximately 0.5 mm two domains are obtained with bowed disclination lines separating the domains. For example, if a small amount of a typical chiral dopant, such as CB15 (**46**) is added to E7, then two

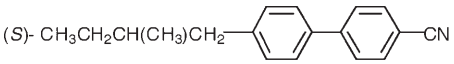

CB15 (**46**)

domains are obtained but the disclination lines between the left- and right-handed domains are curved (Figure 35). The bowing will be related to the enantiomeric excess.

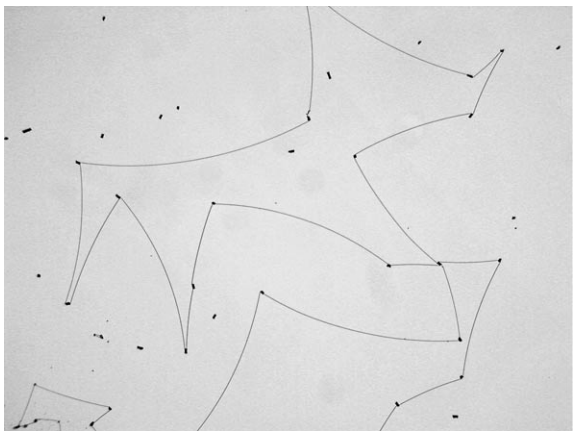

Figure 35. Bowed disclination lines in a TN device containing E7 doped with 0.0027 wt% of CB15, resulting in a pitch of 0.4 mm, (magnification: ×100). The black dots are the spacers which are used to separate the cell surfaces.

Through making reasonable approximations it can be shown that the radius of curvature, R, is related to the pitch length, P, of the chiral nematic material by Equation (1). In

$$P = 2R \quad (1)$$

ideal circumstances, pitch lengths up to 50 mm can be measured, which is equivalent to adding as little as 0.0002 wt% of CB15. Interestingly, CB15 is one of the typical chiral dopants used in small concentrations in commercial TN devices to prevent reverse twist domains. As a 1-cm^2 TN device contains between 0.001 to 0.01 g of liquid-crystal material, this means that only small amounts of the dopant (or material under investigation) are required to evaluate the helical twisting power or the enantiomeric excess.

In liquid-crystal systems, at very high and at very low values of the optical purity, unusual phase behavior can be observed, for example, twist grain boundary (TGB) phase and blue phase (BP) formation. However, measurement of the enantiomeric excess at these limits is usually fraught with difficulties. Furthermore, as most liquid crystals do not possess functional groups that can interact or be derivatized, it is difficult to determine enantiomeric excess by the use of chemical shift reagents in NMR spectroscopy, or chiral HPLC, and the materials are not volatile enough for determination of optical purity by chiral GC. The method described allows for the measurement of the enantiomeric excess, particularly at the extreme limits near to 0 and 100% *ee*. Furthermore, through the observation of curved disclination lines, it can be used as a fast and sensitive test for the presence of a small amount of chiral molecules in a supposedly achiral material, and the excess of molecules of one chirality in a supposedly racemic mixture.

Compound **47** provides a good example of qualitative and quantitative probing of a "so-called" racemic material by

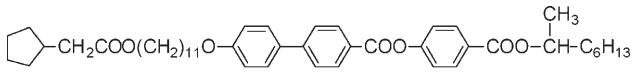

47

liquid-crystalline sensing methods. Compound **47** was initially synthesized from racemic 2-octanol. Subsequently it was also synthesized from prochiral 2-octanone by the synthetic pathway shown in Scheme 9. Material **47** was found to exhibit smectic A and smectic C phases. When placed in a cell with internal ITO coatings and parallel rubbed alignment surfaces, and an electrical voltage applied, the material, while in its smectic C phase, responded as though it were ferroelectric.[96] Figure 36 shows a typical ferroelectric hysteresis loop for

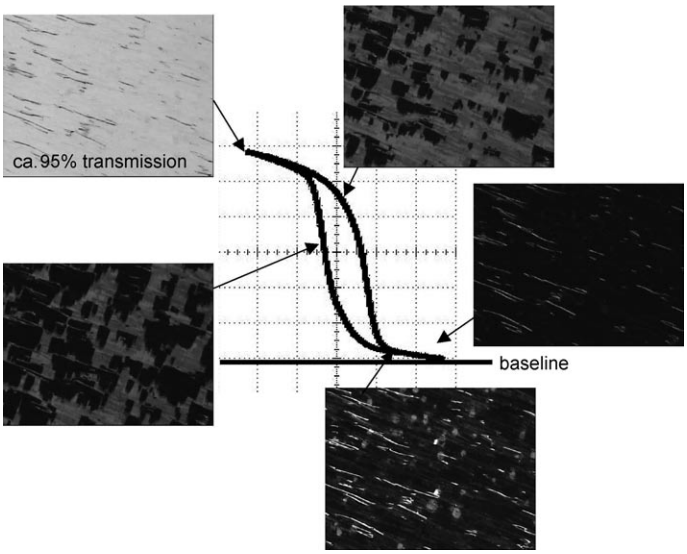

Figure 36. The optical transmission as a function of applied electric field, and the microscopic textures for compound **47** at various points shown on the optical response curve while in its smectic C phase (photomicrographs, magnification: ×100).

transmitted light intensity as a function of the applied field. Figure 36 also shows the defect textures seen in the microscope as the magnitude of the applied electric field is changed, and its direction is reversed. Repetition of the electrical-field experiments, for various examples of **47** synthesized by different routes, yielded the same results. These results lead to the question: how is symmetry breaking occurring for this, and related materials?

The electrical-field results show that compound **47** is ferroelectric, even though the material was synthesized from a racemic starting material. This demonstrates that the material was in an enantiomerically enriched form. However, this

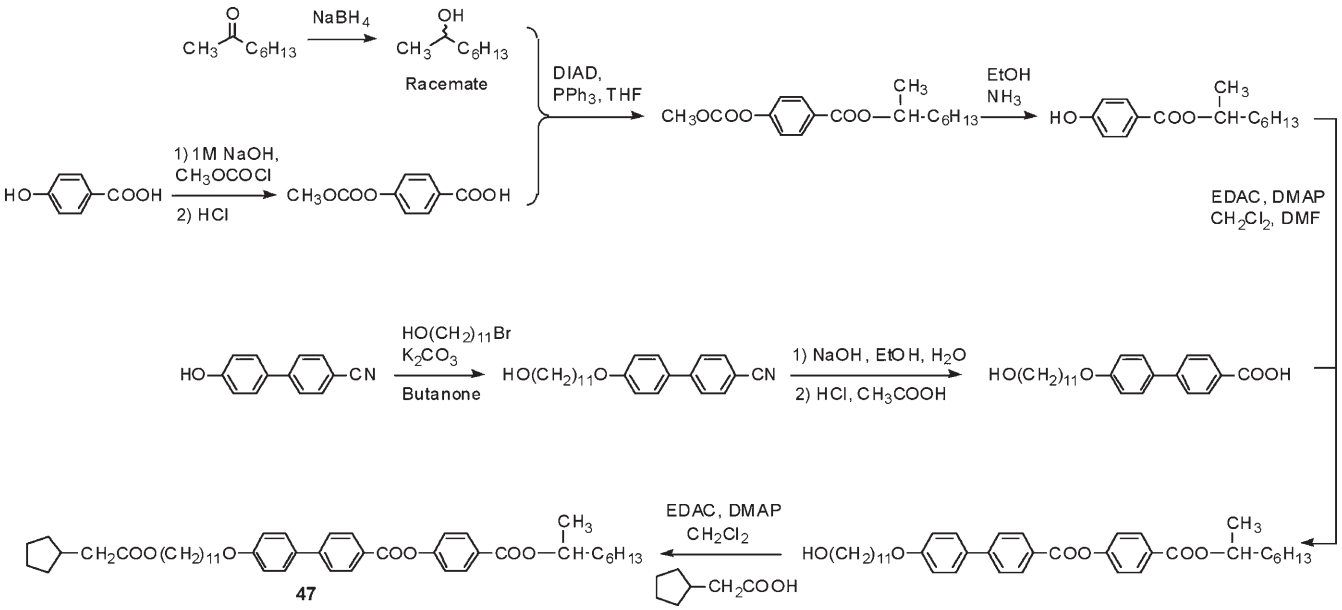

Scheme 9. Synthetic pathway to compound **47**.

experiment does not, and cannot, yield information about the enantiomeric excess because the spontaneous polarization cannot be measured. The hysteresis loop shown in Figure 36 demonstrates that compound **47** is ferroelectric, however, the polarization-reversal method for determining the polarization is not sensitive enough for evaluating very small polarizations. Moreover, the emergence of a spontaneous polarization in liquid crystals is an extrinsic effect that is dominated by the tilt, and thus interactions with the surfaces of the cell and the applied electrical field also need to be taken into account, making it all the more difficult to evaluate small values of the polarization.

However, if we use the TN method of analysis it becomes very clear that compound **47** as synthesized is indeed enantiomerically enriched, and that the enantiomeric excess is in the region of 0.01 % *ee*. This can also be seen when a mixture of **48** (which was prepared by the same method as **47** for the final step, so both materials have commin intermediates) and E7 is cooled from the isotropic liquid (Figure 37;

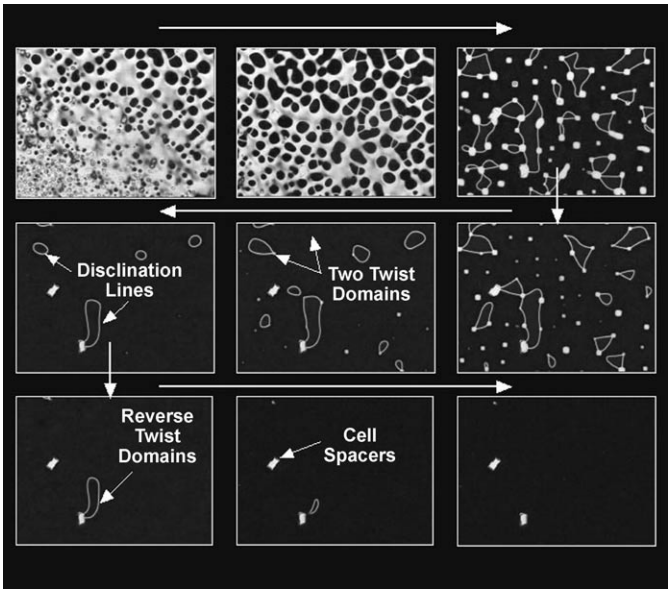

Figure 37. Rapid disappearance of disclination loops on cooling compound **48** from the isotropic liquid in a TN cell under parallel polarizers (magnification: ×100). The long arrows indicate the sequence on cooling.

Cryst 58.4 SmC 77.1 SmA 83.9 °C I). Initially the *schlieren* texture of the nematic phase forms in the bulk, but then it quickly interacts with the surface and two twist domains form. At the outset they are of similar sizes but as the mesophase is cooled to one to two degrees below the clearing point (I to N transition) one twist domain starts to dominate over the other, this process driven by the inequality in the proportions of the two enantiomers present. However, it should be noted that the two domains are not caused by the segregation of the enantiomers. One domain then grows at the expense of the other in the dynamically developing nematic phase until one twist state remains, indicating that the material is not a racemate.

Using other methods, for example chiral GC, it was possible to establish the optical purities of the commercial (*R*)- and (*S*)-2-octanols, and thus the helical twisting power of the (*R*)- and (*S*)-enantiomers of **47** and **48** could be derived.

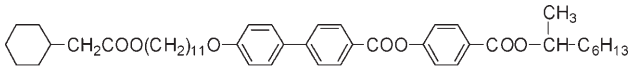

48

By varying the concentrations of the so-called "racemates" of **47** or **48** in a mixture of E7 and examining the curvature of the bowed defects the enantiomeric excess could be determined.[97]

6. Self-Assembly, Self-Organization and Enantioselective Segregation

Thus the methodology described in Section 5 demonstrates how liquid-crystal systems can be used to amplify various effects, in this case chirality, and can act as very sensitive probes in determination of physical properties. However, they can also stabilize unusual structures, and so lastly we turn to liquid crystals where the molecules have unusual shapes, and in particular we will examine the biaxial nematic phase formed by bent-core systems.

The possibility of the occurrence of a biaxial nematic phase Figure 38, was highlighted, in 1970, in an article by Freiser[98] However, it was only as recently as 2004 that

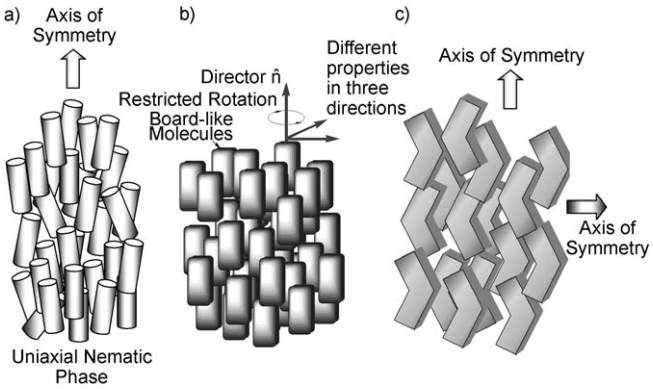

Figure 38. Comparison of the structures of the uniaxial nematic phase (a), and the biaxial nematic phase (b). Representation (c) shows the local structure of the biaxial nematic phase made up of bent-core molecules.

Samulski et al. and Kumar et al.[99] reported low-molecular-mass materials, based on the oxadiazole motif, which exhibited thermotropic biaxial nematic phases. The biaxial order parameter was found to be relatively small, with a value of approximately 0.1. The materials themselves have molecular structures that are bent; the bend being associated with the diphenyloxadiazole moiety located at the center of the aromatic core, as shown by compound **49**. The structures and accompanying phase transitions of a number of diphenyloxadiazoles are shown Scheme 10. Many dissimilarly

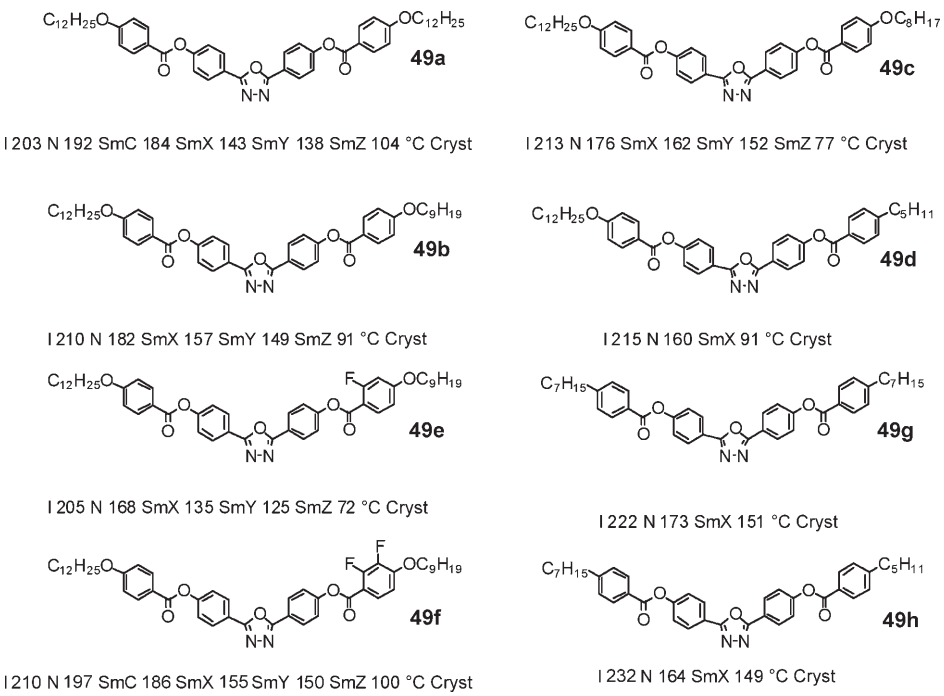

Scheme 10. Structures and phase behavior of some of the compounds **49**.

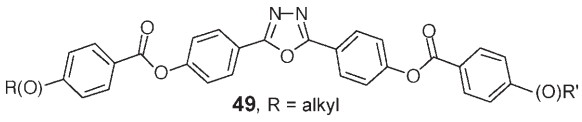

substituted materials with differing aliphatic chain lengths, and fluoro-substituents incorporated in the outer phenyl rings were prepared to moderate and reduce melting points and clearing points, thereby making nematic phases accessible at lower temperatures.[100]

The nematic phase was found to have a broader temperature range for dissimilarly substituted compounds than for the symmetrically substituted parent systems, the only exception being compound **49 f**; the nematic phase transitions were found to occur at lower temperatures, and the melting points were reduced on breaking the symmetry. Scheme 10 also lists the higher ordered, lower temperature, phases which have undefined structures. Following the terminology used by Samulski et al., the unidentified phases are denoted as smectic X, Y, and Z, however it should also be noted that the lettering is not consistent across the series of compounds.

When pristine samples of compound **49 g** were sandwiched between a slide and a cover slip, unusual textures were observed by thermal, polarized-light optical microscopy (POM; Figure 39). On cooling from the isotropic liquid under crossed polarizers, an apparently normal nematic phase was formed first. The nematic phase separated in the form of a *schlieren* texture exhibiting Brownian motion. However, the mesophase also exhibited domains, with walls separating one domain from another. Upon rotation of the analyzer of the microscope the domains which were dark became light and vice versa (see Figure 39). This result indicates the domains are twisted, and that they have the opposite handedness. The dissimilarly substituted diphenyloxadiazoles **49** were also shown to display similar twisted domains.

In investigations of the textures exhibited by compounds **49 g** and **49 h**, intense and extensive dynamical motion in uncovered regions of the nematic phase was observed. Figure 40 shows defect lines in the nematic phase which occur well above the transition to the X phase. At constant temperature well within the temperature range of the nematic phase, defect lines appear and flow rapidly across the *schlieren* texture of the phase, rather like Raleigh–Bernard thermal instabilities.

The results described for the nematic phases of the materials

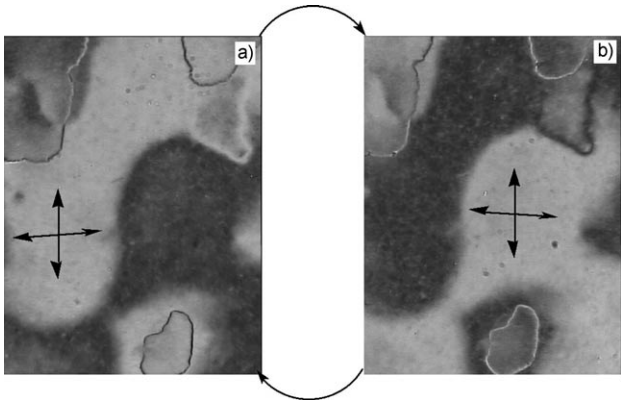

Figure 39. The *schlieren* texture of the nematic phase of compound **49 g** at 222 °C on cooling from the isotropic, where (a) shows an anticlockwise rotation and (b) a clockwise rotation of the analyzer (magnification: ×100).

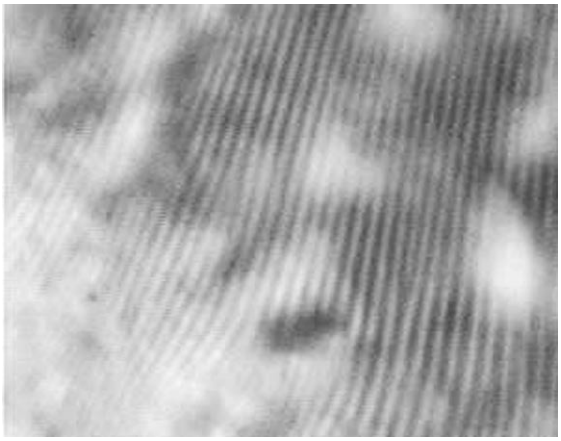

Figure 40. Defect lines of a helical domain in the nematic phase of compounds **49 h** (magnification: ×100).

studied were consistent, with each material exhibiting chiral domains characterized by the formation of a helical macrostructure. In each case the formation of helical domains was dependent on the thermal and mechanical history of the sample, indicating that domain formation was kinetically rather than thermodynamically controlled. Differential scanning calorimetry (DSC) also indicated that there is a thermal event in the liquid state at a temperature slightly above that of the clearing point.

Thus it was possible to speculate on the results in the following way: For the diphenyloxadiazole molecules, chiral conformational isomers, such as **50** and its mirror image,

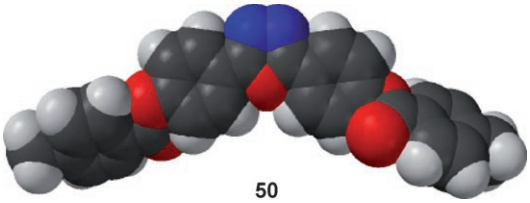

50

might be expected on the bond rotational profile of a molecule. At the clearing point the confomers could self-select to give the most stable self-assembled structure. This situation means that the nucleation of the nematic phase occurs through a process of self-assembly where conformers of one hand pack together to give a helical macrostructure which, in turn, stabilizes confomer formation. Such helical structures would assemble into spiraling ribbons, which then self-organize into chiral nematic phases, and because of the sizes of the ribbons, segregation results in the formation of domains with an excess of one chirality sense.

Figure 41 shows how the self-assembly of chiral conformers, such as **50**, might occur. The chirality of the

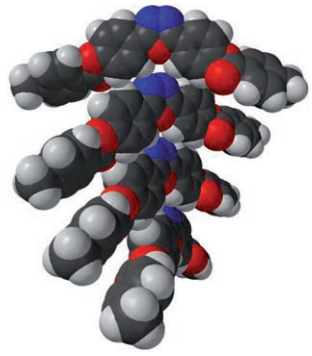

Figure 41. The proposed formation of a helix by the self-assembly of twisted conformers of the bent-core molecules.

conformational structure **50** is generated from the two ester linkages being rotated in opposite directions with respect to the diphenyloxadiazole core. When molecules in this twisted conformation are packed one on top of another a helical self-assembled structure results. The self-organization of the self-assembled structures would result in the formation of a chiral nematic phase. An inverted rotation of the two ester linkages produces the enantiomeric form of conformer **50**, which would assemble to give a helix of opposite handedness. Such self-assembled structures would fluctuate dynamically as a function of time and of external influences, such as surface pinning and mechanical disturbances.

This structural proposal would satisfy the criterion that the process is kinetically driven; and that the energy barrier to conformational flipping is raised through the self-assembly. In addition, helix formation can be suppressed by external forces, such as surface interactions. Furthermore, the length scales of the self-organized structures are such that diffusion probably does not easily occur, thereby stabilizing the formation of domains with an excess of one chirality sense.

The investigations of diphenyloxadiazole materials have shown that the liquid-like achiral nematic phase of these compounds can separate into helical domains of opposite handedness. It was postulated that the domain formation is driven by a self-assembly that creates helical molecular clusters, and accompanies the process of self-organization leading to mesophase formation. Such results are relevant for understanding observations such as compound **49 g** exhibiting a biaxial nematic phase.[99] It has been observed that the large transverse dipole moment associated with the central diphenyloxadiazole unit may be beneficial, if not indispensable, for the exhibition of the biaxial nematic N_b phase. It was argued that the intermolecular associations originating from the large dipole reinforce the transverse orientational correlations that are driven by shape packing of the molecules.[99] Indeed, an atomistic simulation showed the nematic phase of this mesogen to be biaxial.[101] Furthermore, the formation of ferroelectric domains in the nematic phase was found, in which there was a parallel association of the transverse oxadiazole dipoles, that is, the domains are essentially composed of supramolecular aggregates.

Thus it was proposed that the diphenyloxadiazole materials studied could be examples of self-assembling–self-organizing nematogens in which the conformational forms can spontaneously segregate into chiral domains.[100]

Pelzl et al.[102] also reported the formation of chiral domains in the nematic phase of another achiral bent-core system, compound **51** (Cryst 98 (X 80 N 95) °C I). Thus it

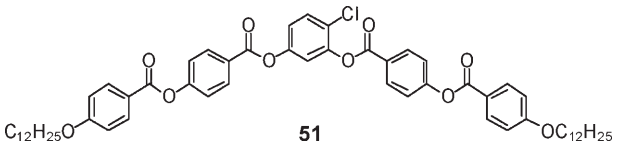

51

appears to be a more general phenomenon that nematic phases of certain achiral materials are capable of exhibiting some form of chiral ordering. In their report, Pelzl et al. also refer to a computer simulation study by Memmer[103] that suggests the helical superstructure occurs as a result of conical twist–bend deformations, and reduces the overall effects arising from flexoelectricity. However, it is also possible to devise a chiral twisted conformer similar to **50** for the bent-core molecule studied by Pelzl et al. This situation emphasizes

again the possibility of self-assembly in a quasi-liquid phase driving enantioselective separations similar to those found in the solid state.

Takezoe et al.[104] also showed that the addition of an achiral bent-core solute to a conventional chiral nematic phase reduces the pitch, thereby indicating that the achiral dopant has a strong chiral effect on the local helical packing of the molecules.

Although it is apparently possible to have enantioselective segregation in the nematic phase of achiral bent-core systems, it is interesting that Strigazzi et al.[105] also evoke a comparable model to explain their observation of chiral domains in the nematic phases of rod-like achiral 4-(alkyloxy)benzoic acids. In this case twisted open dimers formed by hydrogen bonding are the suggested source for the formation of helical structures.[106] Similarly, Jeong et al.[107] found that compound **52** also exhibits a form of chirality. They showed that dimers of **52** were capable of forming chiral propeller

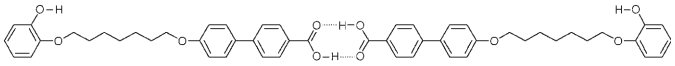

$(\mathbf{52})_2$

architectures leading to helical nematic structures. Thus, as these and Strigazzi's systems form self-assembled structures through hydrogen bonding, it appears that they also have the ability to form chiral macro-self-organized mesophase structures independent of molecular chirality. They are examples of self-assembled, self-organized liquid-crystalline "superphases".

7. Summary

In summary, in this Review an attempt has been made to establish an alternative way of viewing liquid-crystalline self-assembled structures. It has been demonstrated that 1) deformable molecular shapes and topologies of supermolecular and self-assembled supramolecular systems, 2) surface recognition processes of superstructures, and 3) the transmission of those structures and their amplification can lead to unusual mesomorphic behavior where continuum theory is not suitable for their description. The realization that clustering can occur in mesomorphic systems means that the length scales that are normally used to describe liquid crystals are not necessarily valid, that is, mesoscale lengths become more important. This realization is of practical importance in biological systems where mesophases of different cluster types may coexist side by side, for example, cubic and columnar, without the need for a phase transition between the two.

We would like to thank K. J. Toyne, Y. Queneau, R. Deschenaux, G. Mackenzie, P. Boullanger and their respective research groups for their collaborations and contributions to our research. We also thank the EPSRC, SAMPA RTN of the EU, DERA, and the Alliance Programme of the British Council and the Ministere des Affaires Etrangeres, Direction de la Cooperation Scientifique et Technique for financial support.

Received: March 14, 2007
Published online: February 29, 2008

[1] See, for example, *Handbook of Liquid Crystals*, *Vols. 1*, *2a*, *2b and 3* (Eds.: D. Demus, J. W. Goodby, G. W. Gray, H.-W. Spiess, V. Vill), Wiley-VCH, Weinheim, **1998**.
[2] J. L. Ericksen, *Trans. Soc. Rheol.* **1960**, *4*, 29–39; J. L. Ericksen, *Mol. Cryst. Liq. Cryst.* **1969**, *7*, 153 (and Supporting Information therein); J. D. Lee, A. C. Eringen, *J. Chem. Phys.* **1973**, *58*, 4203–4211; J. D. Lee, A. C. Eringen in *Liquid Crystals and Ordered Fluids*, *Vol. 2* (Eds.: J. F. Johnson, R. S. Porter), Plenum, New York, **1974**, pp. 315–330; A. C. Eringen, J. D. Lee in *Liquid Crystals and Ordered Fluids, Vol. 2* (Eds.: J. F. Johnson, R. S. Porter), Plenum, New York, **1974**, pp. 383–402; F. M. Leslie, *Mol. Cryst. Liq. Cryst.* **1969**, *7*, 407 and Supporting Information therein.
[3] F. C. Frank, *Discuss. Faraday Soc.* **1958**, *25*, 19; J. L. Ericksen, *Arch. Ration. Mech. Anal.* **1960**, *4*, 231–237; J. L. Ericksen, *Trans. Soc. Rheol.* **1961**, *5*, 23–24; F. M. Leslie, *Quart. J. Mech. Appl. Math.* **1966**, *19*, 357; F. M. Leslie, *Arch. Ration. Mech. Anal.* **1968**, *28*, 265.
[4] R. B. Meyer, L. Liébert, L. Strzelecki, P. Keller, *J. Phys. Lett.* **1975**, *36*, 69–71.
[5] A. D. L. Chandani, E. Gorecka, Y. Ouchi, H. Takazoe, A. Fukuda, *Jpn. J. Appl. Phys. Part 1* **1989**, *28*, L1265–L1268.
[6] S. Garoff, R. B. Meyer, *Phys. Rev. Lett.* **1977**, *38*, 848–851; S. Garoff, Dissertation, Harvard University, **1977**; R. B. Meyer, *Phys. Rev. Lett.* **1969**, *22*, 918–921.
[7] A. M. Glass, J. W. Goodby, D. H. Olson, J. S. Patel, *Phys. Rev. A* **1988**, *38*, 1673–1675.
[8] J. S. Patel, J. W. Goodby, *Philos. Mag. Lett.* **1987**, *55*, 283–287; J. W. Goodby, E. Chin, J. M. Geary, J. S. Patel, P. L. Finn, *J. Chem. Soc. Faraday Trans. 1* **1987**, *83*, 3429–3446.
[9] *Ferroelectric Liquid Crystals—Principles, Properties and Applications* (Eds.: J. W. Goodby, R. Blinc, N. A. Clark, S. T. Lagerwall, M. A. Osipov, S. A. Pikin, T. Sakurai, K. Yoshino, B. Zeks), Gordon and Breach, Philadelphia, **1991**; S. T. Lagerwall, *Ferroelectric and Antiferroelectric Liquid Crystals*, Wiley-VCH, Weinheim, **2000**.
[10] J. W. Goodby, E. Chin, T. M. Leslie, J. M. Geary, J. S. Patel, *J. Am. Chem. Soc.* **1986**, *108*, 4729–4735; J. W. Goodby, E. Chin, *J. Am. Chem. Soc.* **1986**, *108*, 4736–4742.
[11] J. S. Patel, J. W. Goodby, *Philos. Mag. Lett.* **1987**, *55*, 283–287; J. W. Goodby, E. Chin, J. M. Geary, J. S. Patel, P. L. Finn, *J. Chem. Soc. Faraday Trans. 1* **1987**, *83*, 3429–3446.
[12] R. Bartolino, J. Doucet, G. Durand, *Ann. Phys. (Paris)* **1978**, *3*, 389–395.
[13] M. J. Watson, M. K. Horsburgh, J. W. Goodby, K. Takatoh, A. J. Slaney, J. S. Patel, P. Styring, *J. Mater. Chem.* **1998**, *8*, 1963–1969.
[14] M. P. Neal, M. Solymosi, M. R. Wilson, D. J. Earl, *J. Chem. Phys.* **2003**, *119*, 3567–3573; H. Kamberaj, M. A. Osipov, R. J. Low, M. P. Neal, *Mol. Phys.* **2004**, *102*, 431–446; H. Kamberaj, R. J. Low, M. P. Neal, *Ferroelectrics* **2005**, *315*, 183–196; H. Kamberaj, R. J. Low, M. P. Neal, *Mol. Phys.* **2006**, *104*, 335–357.
[15] J. W. Goodby, D. A. Dunmur, P. J. Collings, *Liq. Cryst.* **1995**, *19*, 703–709.
[16] C. W. Oseen, *Arkiv. Mater. Astron. Fysik* **1923**, *18*, 25; C. W. Oseen, *Arkiv. Mater. Astron. Fysik* **1923**, *18*, 23; C. W. Oseen, *Arkiv. Mater. Astron. Fysik* **1924**, *18*, 36.

[17] E. Bose, *Phys. Z.* **1909**, *10*, 32 – 36; E. Bose, *Phys. Z.* **1909**, *10*, 230 – 244; L. S. Ornstein, F. Zernike, *Phys. Z.* **1918**, *19*, 134 – 137; L. S. Ornstein, *Z. Kristallogr. Kristallgeom.* **1931**, *79*, 90 – 121; L. S. Ornstein, W. Kast, *Trans. Faraday Soc.* **1933**, *29*, 931 – 944.

[18] H. Zocher, V. Birnstein, *Z. Phys. Chem. Abt. A* **1929**, *142*, 113 – 125; H. Zocher in *Liquid Crystals and Plastic Crystals*, *Vol. 1* (Eds.: G. W. Gray, P. A. Winsor), Ellis Horwood, Chichester, **1974**, pp. 64 – 66.

[19] C. Tschierske, *J. Mater. Chem.* **2001**, *11*, 2647 – 2671; T. Kato, N. Mizoshita, K. Kishimoto, *Angew. Chem.* **2006**, *118*, 44 – 74; *Angew. Chem. Int. Ed.* **2006**, *45*, 38 – 68.

[20] I. M. Saez, J. W. Goodby, *J. Mater. Chem.* **2005**, *15*, 26 – 40.

[21] G. R. Newkome, C. D. Weiss, C. N. Moorfield, I. Weiss, *Macromolecules* **1997**, *30*, 2300 – 2304.

[22] S. Sia, I. M. Saez, J. W. Goodby, unpublished results.

[23] I. M. Saez, J. W. Goodby, *Liq. Cryst.* **1999**, *26*, 1101 – 1105.

[24] See, for example, M. W. P. L. Baars, S. Söntjens, H. M. Fischer, H. W. I. Peerlings, E. W. Meijer, *Chem. Eur. J.* **1998**, *4*, 2456 – 2466; S. A. Ponomarenko, N. I. Boiko, V. P. Shibaev, R. M. Richardson, I. J. Whitehouse, E. A. Rebrov, A. M. Muzafarov, *Macromolecules* **2000**, *33*, 5549 – 5558; B. Donnio, J. Barberá, R. Jiménez, D. Guillon, M. Marcos, J.-L. Serrano, *Macromolecules* **2002**, *35*, 370 – 381; J. M. Rueff, J. Barberá, B. Donnio, D. Guillon, M. Marcos, J.-L. Serrano, *Macromolecules* **2003**, *36*, 8368 – 8375; P. Busson, J. Örtegren, H. Ihre, U. W. Gedde, A. Hult, G. Andersson, *Macromolecules* **2001**, *34*, 1221 – 1229.

[25] R. Elsäßer, G. H. Mehl, J. W. Goodby, D. J. Photinos, *Chem. Commun.* **2000**, 851 – 852.

[26] I. M. Saez, J. W. Goodby, *J. Mater. Chem.* **2001**, *11*, 2845 – 2851.

[27] Nobelvortrag: P.-G. de Gennes, *Angew. Chem.* **1992**, *104*, 856 – 859; *Angew. Chem. Int. Ed. Engl.* **1992**, *31*, 842 – 845.

[28] I. M. Saez, J. W. Goodby, R. M. Richardson, *Chem. Eur. J.* **2001**, *7*, 2758 – 2764.

[29] S. Campidelli, T. Brandmüller, A. Hirsch, I. M. Saez, J. W. Goodby, R. Deschenaux, *Chem. Commun.* **2006**, 4282 – 4284.

[30] I. M. Saez, J. W. Goodby, *Chem. Commun.* **2003**, 1726 – 1727; see also *Chem. Eng. News* **2003** (July 14th), p. 10.

[31] J. Ropponen, S. Nummelin, K. Rissanen, *Org. Lett.* **2004**, *6*, 2495 – 2497; I. Bury, B. Heinrich, C. Bourgogne, D. Guillon, B. Donnio, *Chem. Eur. J.* **2006**, *12*, 8396 – 8413.

[32] I. M. Saez, J. W. Goodby, *Chem. Eur. J.* **2003**, *9*, 4869 – 4877.

[33] R. Deschenaux, B. Donnio, D. Guillon, *New J. Chem.* **2007**, *31*, 1064 – 1073; S. Campidelli, C. Eng, I. M. Saez, J. W. Goodby, R. Deschenaux, *Chem. Commun.* **2003**, 1520 – 1521.

[34] F. Brochard, P.-G. de Gennes, *J. Phys.* **1970**, *31*, 691 – 708.

[35] P. E. Cladis, M. Kléman, P. Piéranski, *C. R. Acad. Sci. Paris* **1971**, *273*, 275 – 277.

[36] P. Poulin, N. Frances, O. Mondain-Monval, *Phys. Rev. E* **1999**, *59*, 4384 – 4387.

[37] O. V. Kuksenok, R. W. Ruhwandl, S. V. Shiyanovskii, E. M. Terentjev, *Phys. Rev. E* **1996**, *54*, 5198 – 5203.

[38] R. W. Ruhwandl, E. M. Terentjev, *Phys. Rev. E* **1997**, *55*, 2958 – 2961.

[39] R. W. Ruhwandl, E. M. Terentjev, *Phys. Rev. E* **1997**, *56*, 5561 – 5565.

[40] T. C. Lubensky, D. Pettey, N. Curier, H. Stark, *Phys. Rev. E* **1998**, *57*, 610 – 675.

[41] Y. D. Gu, N. L. Abbott, *Phys. Rev. Lett.* **2000**, *85*, 4719 – 4722.

[42] H. Stark, *Phys. Rev. E* **2002**, *66*, 032701.

[43] P. Poulin, H. Stark, T. C. Lubensky, D. A. Weitz, *Science* **1997**, *275*, 1770 – 1773.

[44] P. Poulin, V. Cabuil, D. A. Weitz, *Phys. Rev. Lett.* **1997**, *79*, 4862 – 4865.

[45] P. Poulin, D. A. Weitz, *Phys. Rev. E* **1998**, *57*, 626 – 637.

[46] O. Mondain-Monval, J. C. Dedieu, T. Gulik-Krzywicki, P. Poulin, *Eur. Phys. J. B* **1999**, *12*, 167 – 170.

[47] P. Poulin, *Curr. Opin. Colloid Interface Sci.* **1999**, *4*, 66 – 71.

[48] J.-C. Loudet, P. Barois, P. Poulin, *Nature* **2000**, *407*, 611 – 613.

[49] M. Kreuzer, T. Tschudi, W. H. De Jeu, R. Eidenshink, *Appl. Phys. Lett.* **1993**, *62*, 1712.

[50] C. Da Cruz, O. Sandre, V. Cabuil, *J. Phys. Chem. B* **2005**, *109*, 14292 – 14299.

[51] M. Zapotocky, L. Ramos, P. Poulin, T. C. Lubensky, D. A. Weitz, *Science* **1999**, *283*, 209 – 212.

[52] V. A. Raghunathan, P. Richetti, D. Roux, *Langmuir* **1996**, *12*, 3789 – 3792.

[53] C. E. Fowler, W. Shenton, G. Stubbs, S. Mann, *Adv. Mater.* **2001**, *13*, 1266 – 1269.

[54] M. Adams, Z. Dogic, S. L. Keller, S. Fraden, *Nature* **1998**, *393*, 349 – 352.

[55] S.-W. Lee, C. B. Mao, C. E. Flynn, A. M. Belcher, *Science* **2002**, *296*, 892 – 895.

[56] I. Musevic, M. Skarabot, U. Tkalec, M. Ravnik, S. Zumer, *Science* **2006**, *313*, 954 – 958.

[57] P. G. Petrov, E. M. Terentjev, *Langmuir* **2001**, *17*, 2942 – 2949.

[58] See, for example, R. Shenhar, T. B. Norsten, V. M. Rotello, *Adv. Mater.* **2005**, *17*, 657 – 669.

[59] See, for example, C. A. Mirkin, R. L. Letsinger, R. C. Mucic, J. J. Storhof, *Nature* **1996**, *382*, 607 – 609; A. P. Alivisatos, K. P. Johnson, X. G. Peng, T. E. T. E. Wilson, C. J. Loweth, M. P. Bruchez, P. G. Schultz, *Nature* **1996**, *382*, 609 – 611; G. Schmid, U. Simon, *Chem. Commun.* **2005**, 697 – 710.

[60] N. Kanayama, O. Tsutsumi, A. Kanazawa, T. Ikeda, *Chem. Commun.* **2001**, 2640 – 2641; I. In, Y.-W. Jun, Y. J. Kim, S. Y. Kim, *Chem. Commun.* **2005**, 800 – 801; L. Cseh, G. Mehl, *J. Am. Chem. Soc.* **2006**, *128*, 13376 – 13377; L. Cseh, G. Mehl, *J. Mater. Chem.* **2007**, *17*, 311 – 315.

[61] S. Kumar, V. Lakshminarayanan, *Chem. Commun.* **2004**, 1600 – 1601; M. Yamada, Z. Shen, M. Miyake, *Chem. Commun.* **2006**, 2569 – 2571.

[62] a) H. Qi, T. Hegmann, *J. Mater. Chem.* **2006**, *16*, 4197 – 4205; b) B. Donnio, P. Garcia Vazquez, J.-L. Gallani, D. Guillon, E. Terazzi, *Adv. Mater.* **2007**, *19*, 3534 – 3539.

[63] Y. Shiraishi, N. Toshima, K. Maeda, H. Yoshikawa, J. Shu, S. Kobayashi, *Appl. Phys. Lett.* **2002**, *81*, 2845 – 2847.

[64] M. Mitov, C. Portet, C. Bourgerette, E. Snoeck, M. Verelst, *Nat. Mater.* **2002**, *1*, 229 – 231.

[65] K. Kanie, T. Sugimoto, *J. Am. Chem. Soc.* **2003**, *125*, 10518 – 10519.

[66] K. Kanie, A. Muramatsu, *J. Am. Chem. Soc.* **2005**, *127*, 11578 – 11579.

[67] M. Draper, J. W. Goodby, I. M. Saez, unpublished results.

[68] M. Bates, *Liq. Cryst.* **2005**, *32*, 1525 – 1529.

[69] J.-M. Lehn in *Supramolecular Chemistry: Concepts and Perspectives*, VCH, Weinheim, **1995**; T. Kato, *Science* **2002**, *295*, 2414 – 2418; J. E. Elemans, A. E. Rowa, R. J. M. Nolte, *J. Mater. Chem.* **2003**, *13*, 2661 – 2670.

[70] G. W. Gray, B. Jones, *J. Chem. Soc.* **1953**, 4179 – 4180; G. M. Bennett, B. Jones, *J. Chem. Soc.* **1939**, 420 – 425; G. W. Gray, B. Jones, *J. Chem. Soc.* **1954**, 683 – 683.

[71] J. D. Bunning, J. W. Goodby, G. W. Gray, J. E. Lydon in *Liquid Crystals of One- and Two-Dimensional Order* (Eds.: W. Helfrich, G. Heppke), Springer, New York, **1980**, pp. 397 – 402; J. E. Bunning, J. E. Lydon, C. Eaborn, P. M. Jackson, J. W. Goodby, G. W. Gray, *J. Chem. Soc. Faraday Trans. 1* **1982**, *78*, 713 – 724.

[72] J. W. Goodby, unpublished results.

[73] Y. Queneau, J. Gagnaire, J. J. West, G. Mackenzie, J. W. Goodby, *J. Mater. Chem.* **2001**, *11*, 2839 – 2844; V. Molinier, P. H. J. Kouwer, Y. Queneau, J. Fitremann, G. Mackenzie, J. W. Goodby, *Chem. Commun.* **2003**, 2860 – 2861; N. Laurent, D.

Lafont, F. Dumoulin, P. Boullanger, G. Mackenzie, P. H. J. Kouwer, J. W. Goodby, *J. Am. Chem. Soc.* **2003**, *125*, 15499 – 15506; F. Dumoulin, D. Lafont, P. Boullanger, G. Mackenzie, G. Mehl, J. W. Goodby, *J. Am. Chem. Soc.* **2002**, *124*, 13737 – 13748; J. W. Goodby, *Mol. Cryst. Liq. Cryst.* **1984**, *110*, 205 – 219; B. Pfannemüller, W. Welte, E. Chin, J. W. Goodby, *Liq. Cryst.* **1986**, *1*, 357 – 370; J. W. Goodby, *Liq. Cryst.* **2006**, *33*, 1229 – 1237.

[74] G. W. Gray in *Liquid Crystals and Plastic Crystals, Vol. 1* (Eds.: G. W. Gray, P. A. Winsor), Ellis Horwood, Chichester, **1974**, pp. 103 – 152; K. J. Toyne in *Thermotropic Liquid Crystals, Critical Reports on Applied Chemistry, Vol. 22* (Ed.: G. W. Gray), Wiley, Chichester, **1987**, pp. 28 – 63.

[75] H. Prade, R. Miethchen, V. Vill, *J. Prakt. Chem.* **1995**, *337*, 427 – 440; J. W. Goodby, *Mol. Cryst. Liq. Cryst.* **1984**, *110*, 205 – 219; E. Barrall, B. Grant, M. Oxsen, E. T. Samulski, P. C. Moews, J. R. Knox, R. R. Gaskill, J. L. Haberfeld, *Org. Coat. Plast. Chem.* **1979**, *40*, 67; R. Miethchen, J. Holz, H. Prade, A. Lipták, *Tetrahedron* **1992**, *48*, 3061 – 3068; V. Vill, T. Böcker, J. Thiem, F. Fischer, *Liq. Cryst.* **1989**, *6*, 349 – 356.

[76] a) Y. Queneau, J. Gagnaire, J. J. West, G. Mackenzie, J. W. Goodby, *J. Mater. Chem.* **2001**, *11*, 2839 – 2844; b) V. Molinier, P. J. H. Kouwer, J. Fitremann, A. Bouchu, G. Mackenzie, Y. Queneau, J. W. Goodby, *Chem. Eur. J.* **2006**, *12*, 3547 – 3557.

[77] B. Pfannemüller, W. Welte, E. Chin, J. W. Goodby, *Liq. Cryst.* **1986**, *1*, 357 – 370; V. Vill, T. Bocker, J. Thiem, F. Fischer, *Liq. Cryst.* **1989**, *6*, 349 – 356; Y. D. Ma, A. Takada, M. Sugiura, A. Fukuda, T. Miyamoto, J. Watanabe, *Bull. Chem. Soc. Jpn.* **1994**, *67*, 346 – 351.

[78] M. A. Marcus, *Mol. Cryst. Liq. Cryst. Lett.* **1986**, *3*, 85 – 89.

[79] S. Fischer, H. Fischer, S. Diele, G. Pelzl, K. Jankowski, R. R. Schmidt, V. Vill, *Liq. Cryst.* **1994**, *17*, 855 – 861.

[80] J. W. Goodby, *Liq. Cryst.* **1998**, *24*, 25 – 38; J. W. Goodby, J. A. Haley, G. Mackenzie, M. J. Watson, V. Ferrieres, D. Plusquellec, *J. Mater. Chem.* **1995**, *5*, 2209 – 2220.

[81] N. Laurent, D. Lafont, F. Dumoulin, P. Boullanger, G. Mackenzie, P. H. J. Kouwer, J. W. Goodby, *J. Am. Chem. Soc.* **2003**, *125*, 15499 – 15506.

[82] S. Bottle, I. D. Jenkins, *J. Chem. Soc. Chem. Commun.* **1984**, 385 – 385.

[83] See, for example, J. F. Kennedy, C. A. White in *Bioactive Carbohydrates*, Wiley, Chichester, **1983**, p. 247.

[84] C. T. Imrie, G. R. Luckhurst in *Handbook of Liquid Crystals, Vol. 2b: High Molecular Weight Liquid Crystals* (Eds.: D. Demus, J. W. Goodby, G. W. Gray, H.-W. Spiess, V. Vill), Wiley-VCH, Weinheim, **1998**, pp. 801 – 833, and references therein.

[85] F. Hardouin, A.-M. Levelut, J. J. Benatter, G. Sigaud, *Solid State Commun.* **1980**, *33*, 337 – 340; F. Hardouin, G. Sigaud, N. H. Tinh, M. F. Achard, *J. Phys. Lett.* **1981**, *42*, 63 – 66.

[86] I. Nishiyama, J. W. Goodby, *J. Mater. Chem.* **1992**, *2*, 1015 – 1023; I. Nishiyama, J. W. Goodby, *J. Mater. Chem.* **1993**, *3*, 149 – 159; J. W. Goodby, *Mol. Cryst. Liq. Cryst.* **1997**, *292*, 245 – 263.

[87] A. Yoshizawa, I. Nishiyama, H. Kikuzaki, N. Ise, *Jpn. J. Appl. Phys. Part 1* **1992**, *31*, L860 – 863; A. Yoshizawa, N. A. Yokoyama, H. Kikuzaki, T. Hirai, *Liq. Cryst.* **1993**, *14*, 513 – 523; A. Yoshizawa, H. Kikuzaki, M. Fukumasa, *Liq. Cryst.* **1995**, *18*, 351 – 366.

[88] K. Miyachi, A. Fukuda in the *Handbook of Liquid Crystals, Vol. 2B: Low Molecular Weight Liquid Crystals II*(Eds.: D. Demus, J. W. Goodby, G. W. Gray, H.-W. Spiess, V. Vill), Wiley-VCH, Weinheim, **1998**, pp. 665 – 691.

[89] P. Mach, R. Pindak, A.-M. Levelut, P. Barois, H. T. Nguyen, H. Baltes, M. Hird, K. J. Toyne, A. J. Seed, J. W. Goodby, C. C. Huang, L. Furenlid, *Phys. Rev. E* **1999**, *60*, 6793 – 6802.

[90] A. Petrenko, J. W. Goodby, *J. Mater. Chem.* **2007**, *17*, 766 – 782.

[91] See, for example, "Thermochromic Cholesteric Liquid Crystals": D. G. MacDonnell in *Thermotropic Liquid Crystals, Critical Reports on Applied Chemistry* (Ed.: G. W. Gray), Wiley, New York, **1987**, pp. 120 – 144.

[92] D. S. Parmar, V. Singh, A. Eftekhari, *Rev. Sci. Instrum.* **1992**, *63*, 225 – 229.

[93] D. M. Walba, D. J. Dyer, J. A. Rego, J. Niessink-Trotter, R. Shao, N. A. Clark, *Ferroelectrics* **2004**, *309*, 121 – 124; D. M. Walba, L. Eshdat, E. Korblova, R. Shao, N. A. Clark, *Angew. Chem.* **2007**, *119*, 1495 – 1497; *Angew. Chem. Int. Ed.* **2007**, *46*, 1473 – 1475.

[94] E. P. Raynes, *Liq. Cryst.* **2006**, *33*, 1215 – 1218.

[95] E. P. Raynes, *Liq. Cryst.* **2007**, *34*, 697 – 699.

[96] S. J. Cowling, A. W. Hall, J. W. Goodby, *Chem. Commun.* **2005**, 1546 – 1548; S. J. Cowling, A. W. Hall, J. W. Goodby, *Adv. Mater.* **2005**, *17*, 1077 – 1080.

[97] S. J. Cowling, E. P. Raynes, J. W. Goodby, in press.

[98] M. J. Freiser, *Phys. Rev. Lett.* **1970**, *24*, 1041.

[99] L. A. Madsen, T. J. Dingemans, M. Nakata, E. T. Samulski, *Phys. Rev. Lett.* **2004**, *92*, 145505; B. R. Acharya, A. Primak, S. Kumar, *Phys. Rev. Lett.* **2004**, *92*, 145506.

[100] V. Görtz, J. W. Goodby, *Chem. Commun.* **2005**, 3262 – 3264.

[101] J. Peláez, M. R. Wilson, *Phys. Rev. Lett.* **2006**, *97*, 267801.

[102] G. Pelzl, A. Eremin, S. Diele, H. Kresse, W. Weissflog, *J. Mater. Chem.* **2002**, *12*, 2591 – 2593.

[103] R. Memmer, *Liq. Cryst.* **2002**, *29*, 483 – 496.

[104] J. Thisayukta, H. Niwano, H. Takezoe, J. Watanabe, *J. Am. Chem. Soc.* **2002**, *124*, 3354 – 3358.

[105] S. I. Torgova, L. Komitov, A. Strigazzi, *Liq. Cryst.* **1998**, *24*, 131 – 141; S. I. Torgova, M. P. Petrov, A. Strigazzi, *Liq. Cryst.* **2001**, *28*, 1439 – 1449.

[106] S. I. Torgova, L. Komitov, A. Strigazzi, *Liq. Cryst.* **1998**, *24*, 131 – 141.

[107] K.-U. Jeong, D.-K. Yang, M. J. Graham, Y. Tu, S.-W. Kuo, B. S. Knapp, F. W. Harris, S. Z. D. Cheng, *Adv. Mater.* **2006**, *18*, 3229 – 3232.